

The impact of chlorine chemistry combined with heterogeneous N₂O₅ reactions on air quality in China

Xiajie Yang^{1,2}, Qiaoqiao Wang^{1,2}, Nan Ma^{1,2}, Weiwei Hu³, Yang Gao⁴, Zhijiong Huang^{1,2}, Junyu Zheng^{1,2}, Bin Yuan^{1,2}, Ning Yang^{1,2}, Jiangchuan Tao^{1,2}, Juan Hong^{1,2}, Yafang Cheng⁵, Hang Su⁵

¹ Institute for Environmental and Climate Research, Jinan University, Guangzhou 511443, China.

² Guangdong-Hongkong-Macau Joint Laboratory of Collaborative Innovation for Environmental Quality, Guangzhou 511443, China.

³ Guangzhou Institute of Geochemistry, Chinese Academy of Sciences, Guangzhou 510640, China.

⁴ Key Laboratory of Marine Environment and Ecology, Ministry of Education, Ocean University of China, Qingdao 266100, China

⁵ Max Planck Institute for Chemistry, Mainz 55128, Germany

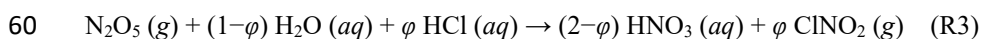
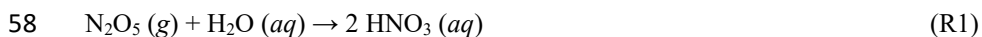
Correspondence to: Qiaoqiao Wang (qwang@jnu.edu.cn)

Abstract: The heterogeneous reaction of N₂O₅ on Cl-containing aerosols (heterogeneous N₂O₅ + Cl chemistry) plays a key role in chlorine activation, NO_x recycling and consequently O₃ and PM_{2.5} formation. In this study, we use the GEOS-Chem model with additional anthropogenic and biomass burning chlorine emissions combined with updated parameterizations for the heterogeneous N₂O₅ + Cl chemistry (i.e. the uptake coefficient of N₂O₅ ($\gamma_{\text{N}_2\text{O}_5}$) and the ClNO₂ yield (φ_{ClNO_2})) to investigate the impacts of chlorine chemistry on air quality in China, the role of the heterogeneous N₂O₅ + Cl chemistry, as well as the sensitivity of air pollution formation to chlorine emissions and parameterizations for $\gamma_{\text{N}_2\text{O}_5}$ and φ_{ClNO_2} . The model simulations are evaluated against multiple observational datasets across China and show significant improvement in reproducing observations of particulate chloride, N₂O₅, and ClNO₂ when including anthropogenic chlorine emissions and updates to the parameterization of the heterogeneous N₂O₅ + Cl chemistry relative to the default model. The simulations show that total tropospheric chlorine chemistry could increase annual mean maximum daily 8-hour average (MDA8) O₃ by up to 4.5 ppbv but decrease PM_{2.5} by up to 7.9 $\mu\text{g m}^{-3}$ in China, 83% and 90% of which could be attributed to the effect of the heterogeneous N₂O₅ + Cl chemistry. The heterogeneous uptake of N₂O₅ on chloride-containing aerosol surfaces is an important loss pathway of N₂O₅ as well as an important source of O₃, and hence is particularly useful in elucidating the commonly seen ozone underestimations relative to observations. The importance of chlorine chemistry largely depends on both chlorine emissions and the parameterizations for the heterogeneous N₂O₅ + Cl chemistry. With the additional chlorine emissions, the simulations show that annual MDA8 O₃ in China could be increased by up to 3.5 ppbv. The corresponding effect on PM_{2.5} concentrations varies largely with regions, with an increase of up to 4.5 $\mu\text{g m}^{-3}$ in the North China Plain but a decrease of up to 3.7 $\mu\text{g m}^{-3}$ in the Sichuan Basin. On the other hand, even with the same chlorine emissions, the effects on MDA8 O₃ and PM_{2.5} in China could differ by 48% and 27%, respectively between different parameterizations.

37 1 Introduction

38 Chlorine (Cl) plays an important role in atmospheric chemistry in both the stratosphere and the
39 troposphere, primarily via the reactions of Cl atom with various atmospheric trace gases including
40 dimethyl sulfide, methane, and other volatile organic compounds (VOCs). The chemistry of Cl is quite
41 similar with that of hydroxyl radicals (OH) while Cl atom reacts up to 2 orders of magnitude faster with
42 some VOCs than OH (Atkinson et al., 2006). Studies have shown that Cl accounts for around 2.5% –
43 2.7% of the global CH₄ oxidation in the troposphere, and the contribution varies across regions, reaching
44 up to 10% – 15% in Cape Verde and ~20% in east China (Lawler et al., 2011; Hossaini et al., 2016). Cl
45 atom, therefore, is regarded as a potentially important tropospheric oxidant.

46 In general, Cl atom can be produced from the photo-dissociation and the oxidation of chlorinated
47 organic species (e.g. CH₃Cl, CH₂Cl₂ and CHCl₃) and inorganic chlorine species (i.e. HCl and Cl₂)
48 (Saiz-Lopez and Von Glasow, 2012; Simpson et al., 2015). Nitryl chloride (ClNO₂), formed through the
49 heterogeneous reaction between dinitrogen pentoxide (N₂O₅) and chloride-containing aerosols
50 (hereinafter referred to as the heterogeneous N₂O₅ + Cl chemistry), is found to be another important
51 source of tropospheric Cl atoms in polluted regions (Liu et al., 2018; Haskins et al., 2019; Choi et al.,
52 2020; Simpson et al., 2015). The heterogeneous formation of ClNO₂ and the subsequent photolysis can
53 be described by reactions R1 – R4 shown below (Finlayson-Pitts et al., 1989; Osthoff et al., 2008). The
54 net reactions of R1 (N₂O₅ hydrolysis on none-chloride-containing aerosols) and R2 (uptake of N₂O₅ on
55 chloride-containing aerosols) could be expressed as R3, in which the ClNO₂ yield (i.e. φ_{ClNO_2} , defined
56 as the molar ratio of produced ClNO₂ to total reacted N₂O₅) represents the fraction of N₂O₅ reacting via
57 R2.



62 Estimates based on model simulations have suggested that ClNO₂ provides a source of Cl atoms totaling

63 0.66 Tg Cl a⁻¹, with the vast majority (95%) being in the Northern Hemisphere (Sherwen et al., 2016).
64 The relative contribution of ClNO₂ to global tropospheric Cl atoms is 14% on average and exhibits clear
65 regional variations (Sherwen et al., 2016). For example, the study by Riedel et al. (2012) reported that
66 the relative contribution is approximately 45% in Los Angeles based on a simple box model combined
67 with local observations.

68 The heterogeneous formation of ClNO₂ also serves as a reservoir for reactive nitrogen at night. The rapid
69 photolysis of ClNO₂ at daytime (R4) not only releases highly reactive Cl atom but also recycles NO₂ back
70 to the atmosphere, which as well significantly affect the daytime photochemistry (Riedel et al., 2014).
71 Previous global and hemispheric models found that the heterogeneous N₂O₅ + Cl chemistry could
72 increase monthly mean values of the maximum daily 8h average (MDA8) O₃ concentrations by 1.0 – 8.0
73 ppbv in most Northern Hemisphere regions (Sarwar et al., 2014; Wang et al., 2019). The reaction also
74 impacts secondary aerosol formation, mainly through the recycling of NO_x (Staudt et al., 2019; Mitroo
75 et al., 2019). For example, Sarwar et al. (2014) estimated that ClNO₂ production decreases nitrate by 3.3%
76 in winter and 0.3% in summer averaged over the entire Northern Hemisphere. The influence of the
77 heterogeneous formation of ClNO₂ in China is even larger due to the polluted environment, leading to an
78 increase in ozone concentrations by up to 7 ppbv, and a decrease in total nitrate by up to 2.35 μg m⁻³ on
79 monthly mean basis (Li et al., 2016; Sarwar et al., 2014)

80 There are two key parameters that determine the uptake efficiency of N₂O₅ and production of ClNO₂, the
81 aerosol uptake coefficient of N₂O₅ ($\gamma_{\text{N}_2\text{O}_5}$) and the ClNO₂ yield (ϕ_{ClNO_2}). The most widely used
82 parameterization for $\gamma_{\text{N}_2\text{O}_5}$ and ϕ_{ClNO_2} was proposed by Bertram and Thornton (2009) (hereinafter referred
83 to as BT09), which is based on the laboratory studies with considerations of aerosol water content,
84 concentrations of nitrate and chloride, and specific surface area (i.e. the ratio of surface area
85 concentrations to particle volume concentrations). However, recent field and model studies have shown
86 that this parameterization would overestimate both $\gamma_{\text{N}_2\text{O}_5}$ and ϕ_{ClNO_2} , especially in regions with high Cl
87 levels (Mcduffie et al., 2018b; Mcduffie et al., 2018a; Xia et al., 2019; Chang et al., 2016; Hong et al.,
88 2020; Yu et al., 2020). The discrepancies could be partly attributed to the complexity of atmospheric
89 aerosols (e.g. mixing state and complex coating materials) in contrast to the simple proxies used in
90 laboratory studies (Yu et al., 2020). Specifically, the suppressive effect of organic coatings is not

91 considered in BT09. Several parameterizations updated from BT09 have been proposed by more recent
92 studies based on field measurements and box model studies (Yu et al., 2020; McDuffie et al., 2018a;
93 McDuffie et al., 2018b; Xia et al., 2019). However, some of these previous field-based parameterizations
94 were derived from observations under different ambient conditions which may not be applicable to the
95 highly polluted regions in China. A full evaluation of the representativeness of different
96 parameterizations for the heterogeneous $\text{N}_2\text{O}_5 + \text{Cl}$ chemistry and the associated impacts on ambient air
97 quality in China is not available yet.

98 In addition to the parameterization, the influence of the heterogeneous $\text{N}_2\text{O}_5 + \text{Cl}$ chemistry is also
99 sensitive to chlorine emissions. In early modelling studies, global tropospheric chlorine is mainly from
100 sea salt aerosols (SSA), and most of the chlorine over continental regions in North America and Europe
101 is dominated by the long-range transport of SSA (Wang et al., 2019; Sherwen et al., 2017). The study by
102 Wang et al. (2019) found an addition of anthropogenic chlorine emissions in the model would result in
103 overestimates of HCl observations in the U.S and suggested insignificant influence of anthropogenic Cl
104 in the U.S. However, there are also studies pointing out the importance of anthropogenic chlorine
105 emissions in China (Le Breton et al., 2018; Yang et al., 2018; Hong et al., 2020). The study by Wang et
106 al. (2020b) suggested that anthropogenic chlorine emissions in China are more than 8 times higher than
107 those in the U.S., and could dominate reactive chlorine in China, resulting in an increase in $\text{PM}_{2.5}$ and
108 Ozone by up to $3.2 \mu\text{g m}^{-3}$ and 1.9 ppbv on annual mean basis, respectively. The comprehensive effects
109 of anthropogenic chlorine on air quality as well as their sensitivities to different parameterizations for
110 the heterogeneous $\text{N}_2\text{O}_5 + \text{Cl}$ chemistry, however, has not been investigated in previous studies.

111 In this work, we use the GEOS-Chem model to investigate the impacts of chlorine chemistry including
112 the heterogeneous $\text{N}_2\text{O}_5 + \text{Cl}$ chemistry on air quality in China. Multiple observational data sets,
113 including N_2O_5 , ClNO_2 , O_3 , $\text{PM}_{2.5}$ and its chemical compositions from different representative sites
114 across China, are used to assess the model performance. With comprehensive chlorine emissions as well
115 as appropriate parameterizations for the heterogeneous $\text{N}_2\text{O}_5 + \text{Cl}$ chemistry, our objectives are: 1) to
116 improve the model's performance regarding the simulation of particulate chloride, ClNO_2 , N_2O_5 , $\text{PM}_{2.5}$
117 and O_3 concentrations; and 2) to extend the investigation on the effects of chlorine chemistry on both
118 $\text{PM}_{2.5}$ and ozone pollution in China as well as their sensitivities to anthropogenic chlorine emissions and

119 the parameterizations for the heterogeneous $\text{N}_2\text{O}_5 + \text{Cl}$ chemistry.

120 **2 Methodology**

121 **2.1 GEOS-Chem Model**

122 The GEOS-Chem model (version 12.9.3, <http://www.geos-chem.org>, DOI: 10.5281/zenodo.3974569) is
123 driven by assimilated meteorological fields GEOS-FP from the NASA Global Modeling and Assimilation
124 Office (GMAO) at NASA Goddard Space Flight Center. The simulation in this study was conducted in
125 a nested-grid model with a native horizontal resolution of $0.25^\circ \times 0.3125^\circ$ (latitude \times longitude) and 47
126 vertical levels over East Asia ($70^\circ - 140^\circ$ E, 15° S – 55° N). The dynamical boundary conditions were
127 from a global simulation with a horizontal resolution of $2^\circ \times 2.5^\circ$. We initialized the model with a 1-month
128 spin up followed by a 1-year simulation for 2018. The simulation included a detailed representation of
129 coupled NO_x – ozone – VOCs – aerosol – halogen chemistry (Sherwen et al., 2016; Wang et al., 2019).
130 Previous studies have demonstrated the ability of GEOS-Chem to reasonably reproduce the magnitude
131 and seasonal variation of surface ozone and particulate matter over East Asia and China (Wang et al.,
132 2013; Geng et al., 2015; Li et al., 2019).

133 **2.1.1 Chlorine Chemistry**

134 The GEOS-Chem model includes a comprehensive chlorine chemistry mechanism coupled with bromine
135 and iodine chemistry. Full details could be found in the study of Wang et al. (2019). Briefly, the model
136 includes 12 gas-phase inorganic chlorine species (Cl , Cl_2 , Cl_2O_2 , ClNO_2 , ClNO_3 , ClO , ClOO , OCIO ,
137 BrCl , ICl , HOCl , HCl), 3 gas-phase organic chlorine (CH_3Cl , CH_2Cl_2 , CHCl_3), and aerosol Cl^- in two
138 size bins (fine mode with radius $\leq 0.5 \mu\text{m}$ and coarse mode with radius $> 0.5 \mu\text{m}$). The gas-aerosol
139 equilibrium between HCl and Cl^- is calculated with ISORROPIA II (Fountoukis and Nenes, 2007) as
140 part of the $\text{H}_2\text{SO}_4 - \text{HCl} - \text{HNO}_3 - \text{NH}_3$ – non-volatile cations (NVCs) thermodynamic system, where
141 Na^+ is used as a proxy for NVCs.

142 The heterogeneous uptake of N_2O_5 on aerosol surfaces leading to the production of ClNO_2 and HNO_3
143 has also been included in GEOS-Chem with the parameterizations for $\gamma_{\text{N}_2\text{O}_5}$ and ϕ_{ClNO_2} proposed by

144 McDuffie et al. (2018b; 2018a) by default (hereinafter referred to as McDuffie parameterization).
 145 McDuffie parameterization is the first field-based empirical parameterization derived from the
 146 framework proposed in multiple laboratory studies including BT09 (Anttila et al., 2006; Bertram and
 147 Thornton, 2009; Riemer et al., 2009) to account for the uptake dependence on aerosol water and nitrate
 148 concentrations as well as the resistance from an organic coating. The coefficients for McDuffie
 149 parameterization were derived from applying a box model to observations of N₂O₅, ClNO₂, O₃, and NO_x
 150 mixing ratios during the winter in the eastern U.S. The parameterization for $\gamma_{\text{N}_2\text{O}_5}$ accounts for both the
 151 inorganic and organic aerosol components and can be described by Eq. 1 – 3:

$$152 \quad \frac{1}{\gamma_{\text{N}_2\text{O}_5}} = \frac{1}{\gamma_{\text{core}}} + \frac{1}{\gamma_{\text{coat}}} \quad \text{Eq. 1}$$

$$153 \quad \gamma_{\text{core}} = \frac{4V}{c \cdot S_a} K_H \times 2.14 \times 10^5 \times [\text{H}_2\text{O}] \left(1 - \frac{1}{k_a \frac{[\text{H}_2\text{O}]}{[\text{NO}_3^-]} + 1} \right) \quad \text{Eq. 2}$$

$$154 \quad \gamma_{\text{coat}} = \frac{4RT\varepsilon H_{\text{aq}} D_{\text{aq}} R_c}{c l R_p} \quad \text{Eq. 3}$$

155 Where γ_{core} represents the reactive uptake of inorganic aerosol core and γ_{coat} represents the retardation of
 156 the organic coating; c is the average gas-phase thermal velocity of N₂O₅ (m s⁻¹), V is the total particle
 157 volume concentration (m³ m⁻³), S_a is the total particle surface area concentration (m² m⁻³), K_H is the
 158 unitless Henry's law coefficient for N₂O₅ with a constant value of 51, [H₂O] and [NO₃⁻] are the
 159 concentrations of aerosol liquid water content and aerosol nitrate (mol L⁻¹), respectively, and k_a is the
 160 rate constant ratio representing the competition between aerosol-phase H₂O and NO₃⁻ for the
 161 H₂ONO₂⁺(aq) intermediate and is fixed at 0.04 in Eq.2; R is the ideal gas constant, T is the temperature
 162 (K), H_{aq} and D_{aq} are the aqueous Henry's law constant and aqueous-phase diffusion coefficient of N₂O₅,
 163 respectively, ε is a linear combination of relative humidity (RH) and O:C ratio (= 0.15 × O:C + 0.0016 ×
 164 RH), and R_p , R_c , and l are the total particle radius, inorganic core radius and organic coating thickness,
 165 respectively (m).

166 φ_{ClNO_2} is calculated following BT09, but is reduced by 75% based on the observations conducted in
 167 eastern U.S. and offshore in spring 2015 (i.e. the WINTER aircraft campaign) (McDuffie et al., 2018b).
 168 It could be described by Eq. 4:

$$169 \quad \varphi_{\text{ClNO}_2} = 0.25 \times \left(k_c \frac{[\text{H}_2\text{O}]}{[\text{Cl}^-]} + 1 \right)^{-1} \quad \text{Eq. 4}$$

170 Where k_c is the rate constant ratio representing the competition between aerosol-phase H_2O and Cl^- for
 171 the $\text{H}_2\text{ONO}_2^+(\text{aq})$ intermediate and is fixed at 1/450 here, and $[\text{Cl}^-]$ is the concentration of aerosol chloride
 172 (mol L^{-1}). For more detailed description of McDuffie parameterization, readers are referred to McDuffie
 173 et al. (2018b; 2018a). Keep it in mind that the coefficients for the parameterizations in Eq. 1 – 4 were
 174 derived to better reproduce wintertime observations in the eastern U.S. However, there are large
 175 uncertainties in both the values of the coefficients and functional form of the parameterizations,
 176 specifically related to their applicability to other regions.

177 Recently, Yu et al. (2020) proposed new parameterizations of $\gamma_{\text{N}_2\text{O}_5}$ and φ_{ClNO_2} based on BT09 to account
 178 for the dependence on aerosol water, nitrate, and chloride concentrations but with coefficients derived
 179 from uptake coefficients directly measured on ambient aerosol in two rural sites in China. The
 180 parameterizations of $\gamma_{\text{N}_2\text{O}_5}$ and φ_{ClNO_2} (hereinafter referred to as Yu parameterization) are described by
 181 Eq. 5 – 6, respectively:

$$182 \quad \gamma_{\text{N}_2\text{O}_5} = \frac{4V}{c \cdot S_a} K_H \times 3.0 \times 10^4 \times [\text{H}_2\text{O}] \left(1 - \frac{1}{k_a \frac{[\text{H}_2\text{O}]}{[\text{NO}_3^-]} + k_b \frac{[\text{Cl}^-]}{[\text{NO}_3^-]} + 1} \right) \quad \text{Eq. 5}$$

$$183 \quad \varphi_{\text{ClNO}_2} = \left(1 + k_c \frac{[\text{H}_2\text{O}]}{[\text{Cl}^-]} \right)^{-1} \quad \text{Eq. 6}$$

184 Where k_b is the rate constant ratio representing the competition between aerosol-phase Cl^- and NO_3^- for
 185 the $\text{H}_2\text{ONO}_2^+(\text{aq})$ intermediate and is fixed at 3.4. In contrast to McDuffie parameterization, k_a and k_c in
 186 Yu parameterization are fixed at 0.033 and 1/150, respectively.

187 Although both the two parameterizations are developed based on BT09, there exist significant differences
 188 of $\gamma_{\text{N}_2\text{O}_5}$ and φ_{ClNO_2} between McDuffie and Yu parameterizations. For $\gamma_{\text{N}_2\text{O}_5}$, McDuffie parameterization
 189 generally follows BT09 for the calculation of the uptake on inorganic aerosols (i.e. γ_{core}), but excludes
 190 the dependence on aerosol chloride so as to better reproduce observed wintertime reactive nitrogen in
 191 eastern U.S. Moreover, the parameterization accounts for the suppressive effects of the organics (i.e. γ_{coat}),
 192 which is not directly included in BT09 (Anttila et al., 2006; Riemer et al., 2009; Morgan et al., 2015). In
 193 contrast to McDuffie parameterization, Yu parameterization excludes the organic suppression but
 194 includes the chloride enhancement so as to better reproduce $\gamma_{\text{N}_2\text{O}_5}$ observed in China (Yu et al., 2020). It
 195 is worth mentioning that the coefficients applied in the parameterization of $\gamma_{\text{N}_2\text{O}_5}$ also differ between
 196 McDuffie and Yu parameterizations as both are fixed to reproduce the ambient observation representing

197 different pollution conditions. For example, k_a is equal to 0.04 in Eq. 2 but 0.033 in Eq. 5. The $\gamma_{\text{N}_2\text{O}_5}$ in
198 McDuffie parameterization is thus expected to be lower compared with the Yu parameterization due to
199 the resistance from organic coating and the lack of the chloride enhancement. For φ_{ClNO_2} , both the
200 McDuffie and Yu parameterizations are based on BT09, but with different coefficients (i.e. $k_c = 1/450$ in
201 Eq. 4 and $1/150$ in Eq. 6). Although k_c in Eq. 4 is relatively smaller, the scaling factor of 0.25 applied in
202 Eq. 4 ultimately results in a much smaller φ_{ClNO_2} in McDuffie parameterization compared with Yu
203 parameterization under the same condition. Again, keep it in mind that McDuffie parameterization is
204 derived from fits to observations over the eastern U.S. (McDuffie et al., 2018a) while Yu parameterization
205 is fitted to observations at rural locations in China (Yu et al., 2020).

206 In this study, we updated the parameterizations for $\gamma_{\text{N}_2\text{O}_5}$ and φ_{ClNO_2} in the heterogeneous $\text{N}_2\text{O}_5 + \text{Cl}$
207 chemistry (hereinafter referred to as parameterizations for heterogeneous $\text{N}_2\text{O}_5 + \text{Cl}$ chemistry) in the
208 GEOS-Chem with Yu parameterization. Additional simulation cases were also performed to evaluate the
209 representativeness of both Yu and McDuffie parameterizations regarding the simulation of N_2O_5 , ClNO_2 ,
210 O_3 , $\text{PM}_{2.5}$ and its chemical compositions in China. Detailed description of the model setup for related
211 cases is provided below in Section 2.1.3.

212 **2.1.2 Emissions**

213 The study uses the Hemispheric Transport of Air Pollution (HTAPv2, <http://www.htap.org/>) based on the
214 emission of 2010 as a global anthropogenic inventory. This inventory is overwritten by a regional
215 emission inventory MIX (with a horizontal resolution of $0.25^\circ \times 0.25^\circ$) over East Asia based on the
216 emission in 2017, which is developed for the Model Inter-Comparison Study for Asia (MICS-Asia) and
217 covers all major anthropogenic sources in 30 Asian countries and regions (Li et al., 2017). In addition,
218 anthropogenic emissions of black carbon (BC) and organic carbon (OC) in Guangdong province, China
219 ($109^\circ - 117^\circ \text{ E}$, $20^\circ - 26^\circ \text{ N}$) are overwritten by a more recent high-resolution inventory ($9 \text{ km} \times 9 \text{ km}$)
220 described by Huang et al. (2021). Biomass burning emissions are from the Global Fire Emissions
221 Database (GFED4) (Van et al., 2010) with a 3-hour time resolution. And the biogenic emissions of VOCs
222 are calculated based on the Model of Emissions of Gases and Aerosols from Nature (MEGAN2.1)
223 (Guenther et al., 2006).

224 Table 1 lists Cl emissions from all sources in the model. The global tropospheric chlorine by default in
225 the model is mainly from the mobilization of Cl^- from SSA distributed over two size bins (fine and coarse
226 modes) (Wang et al., 2019), which is computed online as the integrals of the size-dependent source
227 function depending on wind speeds and sea surface temperatures (Jaeglé et al., 2011). During the
228 simulation year of 2018, SSA contributes 6.5×10^4 Gg Cl^- , most of which however are distributed over
229 the ocean due to its relatively short lifetime (~ 1.5 days) (Choi et al., 2020). The release of atomic Cl
230 from organic chlorine (CH_3Cl , CH_2Cl_2 and CHCl_3) via the oxidation by OH and Cl is also included in
231 the model by default. These organic chlorine gases are mainly of biogenic marine origin (Simmonds et
232 al., 2006), with a mean tropospheric lifetime longer than 250 days (Wang et al., 2020b), and are simulated
233 in the model by imposing fixed surface concentrations as described by Schmidt et al. (2016). Total
234 emissions of Cl atom from CH_3Cl , CH_2Cl_2 , and CHCl_3 are calculated to be 3.8, 2.4, and 0.70 Gg Cl a^{-1} ,
235 respectively.

236 Considering the importance of anthropogenic chlorine in China, we have further updated chlorine
237 inventories in the model to account for anthropogenic HCl, Cl_2 and fine particulate Cl^- , as well as biomass
238 burning HCl and Cl^- emissions (also shown in Table 1 and S1). For fine particulate Cl^- from both
239 anthropogenic and biomass burning, the emissions are estimated based on $\text{PM}_{2.5}$ emissions from MIX
240 and GFED4 inventories combined with the emission ratios of fine particulate Cl^- versus $\text{PM}_{2.5}$ for
241 different emission sectors adopted from the study of Fu et al. (2018). Estimated Cl^- emissions from
242 anthropogenic and biomass burning are 379 and 120 Gg, respectively, comparable to the results of 486
243 Gg in total for the year of 2014 by Fu et al. (2018). The anthropogenic emissions of HCl and Cl_2 are from
244 ACEIC (Anthropogenic Chlorine Emissions Inventory for China) (Liu et al., 2018) and are estimated to
245 be 218 and 8.9 Gg Cl in China, respectively. For HCl from biomass burning, the emission factors from
246 Lobert et al. (1999) are used for different types of biomass provided in GFED4, and a total emission of
247 30 Gg Cl is obtained in China in 2018. Total implemented chlorine emission for the simulation year of
248 2018 is 756 Gg Cl.

249 Figure 1 shows the distribution of Cl emissions from the sources mentioned above. Anthropogenic and
250 biomass burning emissions of HCl are concentrated in the Northeast Plain, North China Plain, Yangtze
251 River Delta, and Sichuan Basin, and are up to 320 kg $\text{Cl km}^{-2} \text{a}^{-1}$ in the Sichuan Basin. Emissions of HCl

252 are low in South China, mainly due to the low chlorine content of coal in these regions (Hong et al.,
253 2020). The relative contribution of biomass burning to total HCl emissions in China is 14% on average
254 but could become dominant in the Northeast Plain due to the discrepancies in the spatial distributions of
255 anthropogenic and biomass burning emissions. The anthropogenic Cl₂ emissions have a similar spatial
256 distribution to that of HCl, but are one order of magnitude lower than HCl emissions. The distribution of
257 non-sea salt Cl⁻ emissions is also similar to that of HCl and Cl₂, except that non-sea salt Cl⁻ emissions
258 are also high in Central China. In contrast, emissions of sea salt Cl⁻ (Fig. S1) are mainly distributed over
259 the ocean, implying limited influences over inland due to rapid deposition during transport. The spatial
260 distributions of different organic chlorine sources are similar, with maximums ($\sim 0.5 \text{ kg Cl km}^{-2} \text{ a}^{-1}$) in
261 coastal regions (Fig. S1).

262 2.1.3 Model setup for different simulation cases

263 In this study, we conducted a series of simulation cases to investigate the effects of chlorine chemistry
264 on air quality in China, the role of N₂O₅ – ClNO₂ chemistry, and the associated sensitivities to chlorine
265 emissions as well as the parameterizations for N₂O₅ – ClNO₂ chemistry. Detailed model setup for those
266 cases is listed in Table 2. The Base case is the one with all updates in this study, including additional
267 chlorine sources from anthropogenic and biomass burning emissions as well as N₂O₅ uptake and ClNO₂
268 production represented by Yu parameterization. The NoEm case is conducted with a similar setup as the
269 Base case but only includes chlorine emissions from SSA and organic chlorine sources so as to evaluate
270 the model improvement originated from the updated chlorine emissions through the comparison with the
271 Base case. The McDuffie case is also performed using the McDuffie instead of Yu parameterization for
272 $\gamma_{\text{N}_2\text{O}_5}$ and ϕ_{ClNO_2} while keeping others the same as the Base case so as to evaluate the discrepancies
273 originated from different parameterizations for the heterogeneous N₂O₅ + Cl chemistry.

274 In addition, while keeping others the same as the Base case, the NoHet case sets ϕ_{ClNO_2} to zero (Eq.6)
275 and removes the enhancement of N₂O₅ uptake from aerosol chloride (i.e. [Cl⁻] = 0 in Eq. 5). The
276 comparison between the Base and NoHet cases could thus evaluate the importance of the heterogeneous
277 N₂O₅ + Cl chemistry (i.e., the model sensitivities to a smaller gamma N₂O₅ and zero ClNO₂ production).
278 Similarly, combined with three more sensitivity cases (NoChem, NoEmHet and NoAll, see details in
279 Table 2), the study provides an overall evaluation of the importance of tropospheric chlorine chemistry

280 as well as its sensitivities to chlorine emissions and the parameterizations for the heterogeneous N_2O_5 +
281 Cl chemistry in the model.

282 2.2 Observations

283 Multiple observed data sets were applied in this study to evaluate the performance of GEOS-Chem
284 simulation, including the concentrations of chemical compositions of $\text{PM}_{2.5}$ from three representative
285 sites, located in south (Guangzhou, 23.14° N, 113.36° E), east (Dongying, 37.82° N, 119.05° E) and north
286 (Gucheng, 37.36° N, 115.96° E) China, respectively (Fig. S2). Concentrations of SO_4^{2-} , NO_3^- , NH_4^+ , Cl^-
287 and organic matter (OM) in $\text{PM}_{2.5}$ were measured by High Resolution Time-of-Flight Aerosol Mass
288 Spectrometer (HR-ToF-AMS; Aerodyne Research Inc., USA, Decarlo et al. (2006)) from October 2 to
289 November 18, 2018 (with a time resolution of 1 minute) at Guangzhou site (Chen et al., 2021b), and
290 from March 18 to April 21, 2018 (with a 1-minute time resolution) at Dongying site. Concentrations of
291 these species were measured by an Aerodyne Quadruple Aerosol Chemical Speciation Monitor (ACSM;
292 Aerodyne Research Inc., USA, Ng et al. (2011)) from November 11 to December 18 in 2018, with a time
293 resolution of 2 minutes at Gucheng site (Li et al., 2021).

294 Concentrations of N_2O_5 and ClNO_2 (with a time resolution of 1 minute) were also measured at
295 Guangzhou site by a Chemical Ionization Mass Spectrometer (CIMS, THS Instruments Inc., Atlanta,
296 (Kercher et al., 2009)) from September 25 to November 12 in 2018 (Ye et al., 2021). To have a thorough
297 evaluation of the representativeness of different parameterizations for $\gamma_{\text{N}_2\text{O}_5}$ and ϕ_{ClNO_2} , observations of
298 ClNO_2 and N_2O_5 at six more sites across China from previous studies (see Table S2 and Fig. S2) are also
299 used in this study. It should be noted that model results sampled at those sites for comparison were
300 simulated in the same months but different years while ignoring the uncertainties associated with the
301 interannual variability.

302 In addition, we also use observed hourly data of O_3 and $\text{PM}_{2.5}$ published by the China National
303 Environmental Monitoring Center (CNEMC, <http://www.cnemc.cn/sss/>, last access on June 20, 2021)
304 to evaluate the model's overall performance in China. The network was launched in 2013 as part of the
305 Clean Air Action Plan and includes ~1500 stations located in 370 cities by 2018 (Fig. S2).

306 **3 Results and discussion**

307 **3.1 Improved model performance with updated chlorine emissions and parameterizations for the** 308 **heterogeneous N₂O₅ + Cl chemistry**

309 Figure 2 shows time series of observed and simulated Cl⁻ concentrations at the Guangzhou, Dongying,
310 and Gucheng sites. The observations show the lowest Cl⁻ concentrations at the Guangzhou site ($0.55 \pm$
311 $0.52 \mu\text{g m}^{-3}$), although the site is the closest to the ocean among all three sites, while the highest
312 concentrations ($4.7 \pm 3.3 \mu\text{g m}^{-3}$) are observed at the Gucheng site, away from the sea. Moderate
313 concentrations of Cl⁻ is observed at the Dongying site, around $1.1 \pm 0.82 \mu\text{g m}^{-3}$. The relatively higher
314 concentrations observed inland again suggest the dominance of non-sea salt Cl⁻ in China, as mentioned
315 before in the Introduction.

316 The comparison between observations and simulated results from the NoEm case shows a serious
317 underestimate of Cl⁻ concentrations, with normalized mean bias (NMB) ranging from -96% to -79%,
318 suggesting the missing of significant chlorine sources in addition to sea salt chlorine. In contrast, the
319 Base case with updated chlorine emissions exhibits much higher Cl⁻ concentrations and can successfully
320 reproduce observations, with average concentrations of 0.77 ± 0.54 , 0.71 ± 0.52 , and $4.5 \pm 2.4 \mu\text{g m}^{-3}$
321 (NMB = 39%, -36% and -4.7%) at the Guangzhou, Dongying, and Gucheng sites, respectively. The
322 increase in Cl⁻ concentrations in the Base case compared with the NoEm case is the most significant at
323 the Gucheng site, by a factor of 24 (from 0.19 to $4.5 \mu\text{g m}^{-3}$ on average). The slight underestimates at the
324 Dongying site in the Base case could be to some extent explained by the bias in GFED4, which
325 underestimates emissions from agricultural fires due to their small size and short duration as suggested
326 by the study of Zhang et al. (2020). In spite of that, the model with the Base case well reproduces the
327 overall distribution of the observed particulate chloride concentrations in China. The correlation
328 coefficients (r) between observed and model results at the three sites also increase from -0.05 – 0.61 in
329 the NoEm case to 0.40 – 0.71 in the Base case. The significant improvement in the model performance
330 again suggests sources other than SSA play a key role in Cl⁻ concentrations in China.

331 The comparison between observed and simulated N₂O₅ (Fig. 3a) shows that NMB for the NoEm case are

332 -58%, 150%, 108% and 25% at the Guangzhou, Wangdu, Taizhou and Mount Tai sites, respectively. In
333 contrast, the corresponding NMB for the Base case are much smaller, -57%, 48%, 91% and 18%,
334 respectively. The improvement in the Base case is apparent at most sites, implying that additional
335 chlorine emissions could effectively increase the uptake coefficient of N_2O_5 in Yu parameterization. As
336 shown in Figure S3, although the values of $\gamma_{N_2O_5}$ between the Base and NoEm cases are similar over the
337 ocean, the Base case has relatively higher $\gamma_{N_2O_5}$ over China compared with the NoEm case (0.016 vs.
338 0.014 on annual mean basis). Little improvement is found at the Guangzhou site (-58% in the NoEm case
339 vs. -57% in the Base case). Previous studies also found an underestimation of N_2O_5 in the Pearl River
340 Delta, which could be partly explained by the underestimation of the sources (e.g. NO_2) and/or the
341 overestimation of the sink of N_2O_5 there (Dai et al., 2020; Li et al., 2016).

342 The N_2O_5 results from the McDuffie case, which uses McDuffie parameterization (a default setting in
343 GEOS-Chem, see Section 2.1.1 and 2.1.3) instead of Yu parameterization are also shown in Fig. 3a. The
344 NMB for the McDuffie case are -53%, 154%, 143% and 37% at the Guangzhou, Wangdu, Taizhou and
345 Mount Tai sites, respectively. The comparison between the McDuffie and Base cases indicates that Yu
346 parameterization can reproduce observed N_2O_5 better in China in general, while McDuffie
347 parameterization tends to overestimate N_2O_5 concentrations. The overestimate of N_2O_5 in McDuffie
348 parameterization suggests the potential underestimate in the corresponding $\gamma_{N_2O_5}$. As shown Figure S3,
349 the value of $\gamma_{N_2O_5}$ from the McDuffie case is much smaller than that from the Base case (0.0071 vs. 0.016
350 averaged over China).

351 The underestimate in $\gamma_{N_2O_5}$ from the McDuffie case could to large extent be explained by the suppressive
352 effect of organic coatings (γ_{coat}) as discussed above in Section 2.1.1. The magnitude of the organic
353 suppression is highly dependent on many factors (e.g. organic composition, particle phase state, etc.) and
354 thus remains poorly quantified (Griffiths et al., 2009; Gross et al., 2009; Thornton et al., 2003). Although
355 many studies have shown that organic aerosol can suppress the N_2O_5 uptake (Anttila et al., 2006; Riemer
356 et al., 2009), the level of organic suppression may be overpredicted in currently implemented
357 parameterization attributed to the poorly quantified and/or unknown factors (e.g. Morgan et al. (2015)).
358 For example, some studies found that ignoring the difference between water-soluble and water-insoluble
359 organics may lead to an upper limit for the suppressive effect of organic coatings and consequently an

360 underestimate in the solubility and diffusivity of N_2O_5 in organic matter (Chang et al., 2016; Yu et al.,
361 2020). Although the γ_{coat} in McDuffie parameterization is calculated as a function of organic aerosol O:C
362 ratio and RH (see Eq. 2), which could increase with higher RH and higher O:C ratio, it may still
363 overpredict the suppressive role of organic coatings in China. On the other hand, the study by Yu et al.
364 (2020) found that excluding the organic coating best reproduced uptake coefficients observed in China.
365 In addition, the underestimate in $\gamma_{N_2O_5}$ in McDuffie parameterization in China could also be to some
366 extent explained by the lack of the chloride enhancement (also discussed in Section 2.1.1). It is worth
367 noting that the evaluation here is specific to China and the differences between Yu and McDuffie
368 parameterizations have not been evaluated elsewhere.

369 For the comparison of $ClNO_2$ (Fig. 3b), we use the mean nighttime (excluding the data at local time of
370 10:00 – 16:00) maximum mixing ratio, as suggested by Wang et al. (2019). Observed $ClNO_2$ is high in
371 Guangzhou (1121 pptv) and Wangdu (~ 990 pptv), followed by Changping (~ 500 pptv) and Beijing (~
372 430 pptv). The lowest concentrations are obtained at Mount Tai and Mount TaiMoShan (~ 150 and 120
373 pptv, respectively) due to relatively clean condition at high altitude. The comparison between observed
374 and simulated $ClNO_2$ at different sites also suggests a better model performance for the Base case with
375 NMB in the range of -28% – 22%, compared with the NMB of -77% – -31% and -59% – -36% for the
376 NoEm and McDuffie cases, respectively. The difference in $ClNO_2$ concentrations is mainly associated
377 with distinct ϕ_{ClNO_2} values among different cases. As shown in Figure S4, the value of ϕ_{ClNO_2} is
378 significantly higher in the Base case (0.36 averaged over China) than in the NoEm (0.14) and McDuffie
379 (0.11) cases. The large difference between the NoEm and Base cases again emphasizes the important role
380 of non-sea salt chlorine in the formation of $ClNO_2$. The overall underestimates in McDuffie
381 parameterization on the other hand may suggest that the scaling factor of 0.25 applied to ϕ_{ClNO_2} in Eq. 4
382 is too much for the atmospheric condition in China. More field measurements and model evaluations are
383 required to come up with a more precise parameterization better representing ϕ_{ClNO_2} in China.

384 Overall, with updated chlorine emissions and Yu parameterization for $\gamma_{N_2O_5}$ and ϕ_{ClNO_2} , the Base case
385 agrees better with both the magnitude and the spatial variation of observed N_2O_5 and $ClNO_2$ in China.
386 The differences in $\gamma_{N_2O_5}$ and ϕ_{ClNO_2} could also affect the ratios of $ClNO_2$ to HNO_3 . As shown in Figure
387 S5, the value of $ClNO_2/HNO_3$ is the highest from the Base case (9.8% averaged in China and up to 47%

388 in the Sichuan Basin on annual mean basis), followed by the McDuffie (4.7% averaged in China and up
389 to 18% in the Sichuan Basin) and NoEm (3.1% averaged in China and up to 12% in coastal regions)
390 cases.

391 To further elucidate how the model behaves in reproducing the spatial distribution of ozone and PM_{2.5}
392 through the incorporation of the additional chlorine emissions and Yu parameterization for the
393 heterogeneous N₂O₅ + Cl chemistry, simulated MDA8 O₃ and PM_{2.5} from different cases were compared
394 with observations across China. Figure 4 shows simulated annual mean MDA8 O₃ and PM_{2.5} in 2018 in
395 China from the Base case compared with the observations from CNEMC (China National Environmental
396 Monitoring Center, introduced in Section 2.2). The observed annual mean MDA8 O₃ and PM_{2.5} are 49
397 ppbv and 39 μg m⁻³ respectively in 2018 in China. Model results from the Base case could generally
398 reproduce observed spatial and seasonal variations of annual mean MDA8 O₃ and PM_{2.5} concentrations,
399 with NMB of -26% and 3.6% and *r* of 0.83 and 0.81 respectively (Fig. S6).

400 Table 3 also summarized the model performance on both annual and seasonal scales regarding the
401 simulation of O₃ and PM_{2.5} from different cases. For the comparison with observed MDA8 O₃, although
402 different simulation cases show a similar range of *r*, the Base case tends to have a slightly smaller bias
403 in general, with NMB of -26% on annual average (-49% – -5.5% on seasonal mean) vs. -28% (-54% – -
404 5.9%) in the NoEm and -27% (-53% – -5.2%) in the McDuffie case. For the comparison with observed
405 PM_{2.5}, the NMB bias from the Base case is 3.6% on annual average (-6.3% – 28% on seasonal mean).
406 Compared with the NoEm case, there is some improvement in summer (5.0% vs. 3.9%) and winter (-
407 7.9% vs. -4.3%) but slightly larger bias in autumn (26% vs. 28%). The McDuffie case on the other hand
408 produces slightly higher PM_{2.5} concentrations, with NMB of 5.6%. Regarding the chemical compositions
409 of PM_{2.5} (Table S3), although the model performance varies with sites and species, the Base case
410 demonstrates better agreement with observations compared with the NoEm and McDuffie cases in
411 general.

412 On the whole, the model performance is better with the additional anthropogenic and biomass burning
413 chlorine emissions combined with Yu parameterization for the heterogeneous N₂O₅ + Cl chemistry.
414 Therefore, the following investigation of the impacts of chlorine chemistry on air quality in China as
415 well as their sensitivities to chlorine emissions and parameterizations for the heterogeneous N₂O₅ + Cl

416 chemistry is mainly based on the Base case.

417 **3.2 Impacts of tropospheric chlorine chemistry on air quality and the role of the heterogeneous** 418 **N₂O₅ + Cl chemistry**

419 To comprehensively quantify the importance of chlorine chemistry, we conducted a sensitivity case in
420 which all related tropospheric chlorine chemistry was turned off (NoChem, also listed in Table 2). The
421 differences between the Base and NoChem cases (Fig. 5 and Fig. S7) could thus represent the impact of
422 the chlorine chemistry. The comparison shows that chlorine chemistry could increase annual mean
423 nighttime max ClNO₂ surface concentrations by 243 pptv averaged in China (up to 1548 pptv in the
424 Sichuan Basin). The increase in annual mean Cl atoms is 1.7×10^3 molec cm⁻³ averaged in China (up to
425 7×10^3 molec cm⁻³ in coastal regions). The increased Cl atoms could react with VOCs (especially alkanes)
426 producing more peroxy radicals, including organic peroxy radicals (RO₂) and hydroperoxyl radicals
427 (HO₂). As shown in Figure S7 (a), the chlorine chemistry could increase annual mean HO₂ concentrations
428 by 1.6×10^6 molec cm⁻³ averaged in China (up to 8.6×10^6 molec cm⁻³ in the coastal regions). In the
429 presence of NO, the peroxy radicals recycle OH while oxidize NO to NO₂. The subsequent photolysis of
430 NO₂ could further lead to more O₃ production and consequently also more OH (Osthoff et al., 2008;
431 Riedel et al., 2014; Simpson et al., 2015). On the other hand, the recycling of NO_x back into the
432 atmosphere associated with the photolysis of ClNO₂ could also lead to more O₃ production. The results
433 here show a significant increase in surface annual mean OH (Fig. S7 (b)) and MDA8 O₃ (Fig. 5c) by 3.8
434 $\times 10^4$ molec cm⁻³ and 1.1 ppbv respectively averaged in China (up to 1.2×10^5 molec cm⁻³ and 4.5
435 ppbv respectively in the Sichuan Basin). In contrast, annual mean PM_{2.5} surface concentrations are
436 decreased by 0.91 μg m⁻³ averaged in China (up to 7.9 μg m⁻³ in the Sichuan Basin), mainly due to the
437 decrease of NO₃⁻ and NH₄⁺ (up to 6.4 μg m⁻³ and 1.9 μg m⁻³ respectively), although SO₄²⁻ concentrations
438 are increased slightly by up to 1.2 μg m⁻³ in the Sichuan Basin (Fig. S7).

439 Both global and regional studies suggested that the heterogeneous N₂O₅ + Cl chemistry can enhance O₃
440 production through the production of Cl atoms and the recycling of NO_x (Li et al., 2016; Sarwar et al.,
441 2014; Wang et al., 2019). Therefore, we further investigate the role that the heterogeneous N₂O₅ + Cl
442 chemistry plays in tropospheric chlorine chemistry through the comparison between the Base and NoHet

443 (Fig. 6 and Fig. S8) cases. Keep it in mind that the comparison is mainly assessing the impact of ClNO₂
444 production, namely the uptake of N₂O₅ on chloride aerosol, not the general role of N₂O₅ heterogeneous
445 chemistry. The comparison illustrates that the heterogeneous N₂O₅ + Cl chemistry could result in a
446 significant production of ClNO₂, reaching 600 – 1400 pptv for annual mean nighttime max surface
447 concentrations in the North China Plain, and up to 1546 pptv in the Sichuan Basin. The change in the
448 surface concentrations of Cl atoms (an annual mean increase of $1 - 4 \times 10^3$ molec cm⁻³ in central and
449 eastern China) is mainly due to the photolysis of ClNO₂ and accounts for 74% of total change in annual
450 mean Cl atoms due to all tropospheric chlorine chemistry in China, which are consistent with the results
451 from the previous study by Liu et al. (2017).

452 In addition to the production of Cl atoms, the ClNO₂ formation also affects the partitioning of NO_y from
453 HNO₃ into more reactive forms (e.g., NO_x and ClNO₂) through the recycling of NO_x, and therefore of
454 great importance in atmospheric chemistry (Bertram et al., 2013; Li et al., 2016; Wang et al., 2020a). To
455 analyze the impact of the heterogeneous N₂O₅ + Cl chemistry on NO_y partitioning, Figure S9 shows the
456 change in the ratios of NO_x to NO_y and NO₃⁻ to NO_y as the difference between the Base and NoHet cases.
457 Since ClNO₂ could be treated as a reservoir for reactive nitrogen at night, we include ClNO₂ as part of
458 NO_x in the calculation (NO_x = NO + NO₂ + ClNO₂ and NO_y = NO + NO₂ + ClNO₂ + HNO₃ + 2 × N₂O₅
459 + NO₃ + HONO + HNO₄ + NO₃⁻ + various organic nitrates). The results show that due to the ClNO₂
460 production, the ratios of NO_x to NO_y increase by 1.8% averaged in China and up to 5.4% in the Sichuan
461 Basin, Northeast Plain and North China Plain on annual mean basis. Meanwhile, the ratios of NO₃⁻ to
462 NO_y decrease by 1.1% averaged in China and up to 5.1% in the Sichuan Basin on annual mean basis.

463 Consequently, the annual mean MDA8 O₃ surface concentrations are increased by 1.5 – 3 ppbv in central
464 and eastern China and up to 3.8 ppbv in the Sichuan Basin, accounting for 83% of total change in annual
465 mean MDA8 O₃ due to all tropospheric chlorine chemistry in China. It is interesting to note that while
466 MDA8 O₃ surface concentrations show maxima in summer and minima in winter in general, the influence
467 of the heterogeneous N₂O₅ + Cl chemistry on O₃ concentrations exhibits a different seasonality. The
468 increase in seasonal mean MDA8 O₃ concentrations is the largest in winter (by up to 6.5 ppbv in the
469 Sichuan Basin) but is less than 1.5 ppbv in summer. This is because of more accumulation of N₂O₅ and
470 ClNO₂ in dark conditions in long winter nights (Sarwar et al., 2014).

471 There also exhibits an obvious decrease in the annual mean surface concentrations of $PM_{2.5}$ attributed to
472 the heterogeneous $N_2O_5 + Cl$ chemistry, ranging from 1.5 to $4.5 \mu g m^{-3}$ in central and eastern China
473 (accounting for 90% of total change in annual mean $PM_{2.5}$ due to all tropospheric chlorine chemistry in
474 China). The decrease is more significant in autumn and winter in China, with a range of $3.5 - 5.5 \mu g m^{-3}$
475 ³ in central and eastern China and being up to $11 \mu g m^{-3}$ in the Sichuan Basin. In contrast, the decrease in
476 $PM_{2.5}$ is less than $2 \mu g m^{-3}$ in summer in China. The change in $PM_{2.5}$ is mainly due to the decrease in
477 NO_3^- (up to $6.2 \mu g m^{-3}$ in the Sichuan Basin on annual average). In addition, NH_4^+ is also decreased by
478 up to $1.8 \mu g m^{-3}$ in the Sichuan Basin on annual average, following the pattern of ΔNO_3^- . This is because
479 NH_3 is in excess in most regions in China (Xu et al., 2019) and the formation of $ClNO_2$ via R2 could
480 hinder the formation of HNO_3 and shift the partitioning between NH_3 and NH_4^+ towards NH_3 . Unlike the
481 change in NO_3^- and NH_4^+ , the heterogeneous $N_2O_5 + Cl$ chemistry increases surface SO_4^{2-} concentration
482 slightly, which could be explained by the enhancements of atmospheric oxidation associated with the
483 increase in Cl atoms, OH and O_3 , facilitating the formation of secondary aerosols (Sarwar et al., 2014).

484 On the other hand, the effect of tropospheric chlorine chemistry without the heterogeneous $N_2O_5 + Cl$
485 chemistry is much smaller (Fig. S10, the comparison between the NoHet and NoChem cases), leading to
486 an increase of up to 0.7 ppbv in inland China and a decrease of 0.3 – 0.5 ppbv in coastal regions for
487 annual mean MDA8 O_3 concentrations. The increase is probably associated with Cl atoms from
488 photolysis of gas-phase chlorine, especially non-sea salt Cl_2 in inland China, while the decrease at coastal
489 regions is mainly due to catalytic production of bromine and iodine radicals originated from sea-salt
490 aerosols. The comparison demonstrates the dominance of the heterogeneous $N_2O_5 + Cl$ chemistry in
491 total tropospheric chlorine chemistry in China.

492 **3.3 The effect of heterogeneous $N_2O_5 + Cl$ chemistry in response to chlorine emissions**

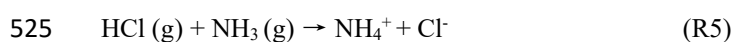
493 Since both $\gamma_{N_2O_5}$ and ϕ_{ClNO_2} in Yu parameterization are highly dependent on $[Cl^-]$, the effect of the
494 heterogeneous $N_2O_5 + Cl$ chemistry on air quality is thus sensitive to chlorine emissions. Figure 7 shows
495 the effects of the additional chlorine emissions from anthropogenic and biomass burning sources on
496 annual mean surface concentrations of different species (Cl^- , Cl atom, OH, MDA8 O_3 , $PM_{2.5}$ and NO_3^-)
497 in China, calculated as the differences between the Base and the NoEm case. With the implementation
498 of the additional chlorine emissions, the particulate Cl^- concentration increased significantly in inland

499 China, with the largest increase in the Sichuan Basin ($4.5 \mu\text{g m}^{-3}$) and little change in west China. The
500 increase is in the range of $1.5 - 3.5 \mu\text{g m}^{-3}$ in the North China Plain and $< 0.5 \mu\text{g m}^{-3}$ in South China. The
501 spatial distribution of ΔCl atoms is also consistent with that of the additional chlorine emissions and ΔCl ,
502 showing the largest increment in the Sichuan Basin (about $4.5 - 5 \times 10^3 \text{ molec cm}^{-3}$). There is also a
503 moderate increase in Cl atoms in the Northeast Plain and North China Plain, with a range of $1.5 - 4 \times$
504 $10^3 \text{ molec cm}^{-3}$. Only a minor increase of Cl atoms is found in South China ($< 1 \times 10^3 \text{ molec cm}^{-3}$).

505 As discussed earlier in Section 3.2, increased Cl atoms could lead to more HO_2 and OH via VOCs
506 oxidation. Combined with increased NO_x associated with the release of NO_2 upon the photolysis of
507 ClNO_2 , further increases in both O_3 and OH could also be expected. The increase in OH is around $2 - 9$
508 $\times 10^4 \text{ molec cm}^{-3}$ in central and eastern China on annual mean basis. The increase in MDA8 O_3 surface
509 concentrations ranges from 0.5 to 3 ppbv in central and eastern China and reaches up to 3.5 ppbv in the
510 Sichuan Basin on annual average. The impacts of chlorine sources on O_3 formation also vary with seasons.
511 Although O_3 pollution is generally severe in summer, the change in MDA8 O_3 due to the additional
512 chlorine sources is relatively minor, with maxima of 0.7 ppbv in the Sichuan Basin and < 0.5 ppbv in
513 most other regions averaged in summer. In contrast, the increase is most obvious in winter, with maxima
514 of 5.2 ppbv in the Sichuan Basin on seasonal average.

515 The effects of the additional chlorine emissions on surface $\text{PM}_{2.5}$ concentrations are complicated. The
516 North China Plain shows the largest increase ($3 - 4.5 \mu\text{g m}^{-3}$ on annual average), mainly due to the
517 increase in Cl^- , which could also promote the heterogeneous $\text{N}_2\text{O}_5 + \text{Cl}$ chemistry and lead to more NO_3^-
518 production (Chen et al., 2021a). In contrast, the Sichuan Basin exhibits both an increase (by up to $4.2 \mu\text{g}$
519 m^{-3}) and a decrease (by up to $3.7 \mu\text{g m}^{-3}$). The decrease of $\text{PM}_{2.5}$ in the Sichuan Basin is mainly due to the
520 large decrease of NO_3^- there. In the Sichuan Basin, nitrate formation is dominated by the heterogeneous
521 hydrolysis of N_2O_5 (Tian et al., 2019) while the additional Cl^- could hinder the path of N_2O_5 hydrolysis
522 due to the competition with the path of ClNO_2 formation. Consequently, the additional chlorine emissions
523 result in a decrease of NO_3^- up to $5.6 \mu\text{g m}^{-3}$ in the Sichuan Basin on annual average.

524 In addition, NH_4^+ concentrations could also be affected through the reaction of R5:



526 In the Northeast Plain and North China Plain where anthropogenic and biomass burning emissions of

527 HCl are high, the annual mean NH_4^+ surface concentrations are increased by $0.5 - 1.5 \mu\text{g m}^{-3}$ (Fig. S11
528 (a)). NH_4^+ concentrations are also affected by the gas-particle partitioning equilibrium, and decrease as
529 the pH value gets higher (or increase with H^+ concentrations). Therefore, the competition between the
530 heterogeneous $\text{N}_2\text{O}_5 + \text{Cl}$ chemistry and N_2O_5 hydrolysis could also affect the formation of NH_4^+ . In
531 other words, increased Cl^- concentrations could result in less H^+ and thus less NH_4^+ . Consequently, there
532 also exists some decrease in NH_4^+ concentrations in the Sichuan Basin associated with the large decrease
533 in NO_3^- concentrations. In contrast, little change is found for surface SO_4^{2-} concentrations, less than 0.5
534 $\mu\text{g m}^{-3}$ in most regions of China (Fig. S11 (b)).

535 It is worth mentioning that the effects of the additional chlorine emissions work mainly through the
536 heterogeneous $\text{N}_2\text{O}_5 + \text{Cl}$ chemistry. Without this heterogeneous chemistry, the increase of chlorine
537 emissions shows only a minor change in Cl atoms ($< 10^3 \text{ molec cm}^{-3}$ in China, estimated as the difference
538 between the NoHet and NoEmHet cases in Fig. S12). The impact of chlorine emissions on O_3
539 concentrations also weakens when the heterogeneous $\text{N}_2\text{O}_5 + \text{Cl}$ chemistry is turned off, with an increase
540 of $0.5 - 1$ ppbv in MDA8 O_3 on annual average (vs. $0.5 - 3$ ppbv mentioned above).

541 On the other hand, the impacts of heterogeneous $\text{N}_2\text{O}_5 + \text{Cl}$ chemistry on air quality in inland China
542 would be seriously underestimated if the additional anthropogenic and biomass burning chlorine sources
543 are ignored. If only sea salt chlorine emission is included in the simulation, the increase of ClNO_2 surface
544 concentrations resulted from heterogeneous $\text{N}_2\text{O}_5 + \text{Cl}$ chemistry only occurs in coastal regions due to
545 the heterogeneous uptake of N_2O_5 on sea salt chloride aerosols (by up to 260 pptv on annual average,
546 indicated by the difference between the NoEm and NoEmHet cases, Fig. S13). Consequently, the increase
547 in Cl atoms and MDA8 O_3 surface concentrations is found mainly in coastal regions. For instance, annual
548 mean MDA8 O_3 concentrations are increased by up to 2 ppbv in coastal regions, but by less than 0.5
549 ppbv in inland China. In other words, the dominance of the heterogeneous $\text{N}_2\text{O}_5 + \text{Cl}$ chemistry in the
550 impact of chlorine chemistry on air quality in China is to large extent driven by the additional chlorine
551 emissions.

552 **3.4 The effect of heterogeneous N₂O₅ + Cl chemistry in response to parameterizations for $\gamma_{\text{N}_2\text{O}_5}$ and**

553 ϕ_{ClNO_2}

554 It should be noted that the impact of the heterogeneous N₂O₅ + Cl chemistry on air quality not only
555 depends on the amount of chlorine emissions, but is also sensitive to the parameterizations for $\gamma_{\text{N}_2\text{O}_5}$ and
556 ϕ_{ClNO_2} . As discussed earlier (Fig. 3a), there exists a large difference in simulated N₂O₅ between the Base
557 and NoEm cases at the Wangdu site, implying the sensitivity of $\gamma_{\text{N}_2\text{O}_5}$ to chlorine emissions in Yu
558 parameterization and thus the importance of non-sea salt chlorine emissions in China. This is consistent
559 with the dependence on chloride in Yu parameterization, which is included to better reproduce $\gamma_{\text{N}_2\text{O}_5}$
560 observations in China (Yu et al., 2020). The comparison between the Base and NoHet cases ($\gamma_{\text{N}_2\text{O}_5} =$
561 0.016 and 0.014, respectively) also suggests that the heterogeneous uptake of N₂O₅ on chloride-
562 containing aerosol surfaces in Yu parameterization is an important loss pathway of N₂O₅ and should not
563 be ignored.

564 Unlike Yu parameterization, N₂O₅ concentrations have little dependence on chlorine emissions in
565 McDuffie parameterization (Fig. 3a). This insensitivity to chlorine emissions could be expected from Eq.
566 2 where the dependence on aerosol chloride is not included so as to better reproduce wintertime reactive
567 nitrogen observations in the eastern U.S. The little dependence of $\gamma_{\text{N}_2\text{O}_5}$ on concentrations of Cl⁻ together
568 with the lower value of ϕ_{ClNO_2} make the results from the McDuffie case less sensitive to chlorine
569 emissions, producing less ClNO₂ and Cl atoms compared with the Base case (with Yu parameterization)
570 although with the same emission. Consequently, the McDuffie case produces less O₃, with annual mean
571 surface concentrations of MDA8 O₃ lower by 0.47 ppbv averaged in China (by up to 2 ppbv in the
572 Sichuan Basin), but results in more PM_{2.5} (0.63 $\mu\text{g m}^{-3}$ averaged in China and up to 4.7 $\mu\text{g m}^{-3}$ in the
573 Sichuan Basin on annual mean basis mainly due to changes in NO₃⁻) (Fig. 8). In other words, compared
574 to the Base case with Yu parameterization, the impacts of chlorine emissions on annual MDA8 O₃ and
575 PM_{2.5} in the McDuffie case has been decreased by 48% and 27% respectively averaged in China.
576 Therefore, even with the same amounts of chlorine emissions, the impacts of the heterogeneous N₂O₅ +
577 Cl chemistry on air quality vary significantly with different parameterizations.

578 4 Conclusions

579 Considering the importance of chlorine chemistry in modulating the O₃ and PM_{2.5} as well as the
580 previously ignored chlorine emission from anthropogenic and biomass burning, we updated the GOES-
581 Chem model in this study with comprehensive chlorine emissions and a new parameterization based on
582 the study of Yu et al. (2020) for the heterogeneous N₂O₅ + Cl chemistry, followed by the extensive
583 evaluation of model performance. Through the utilization of a large number of observational datasets,
584 we found a substantial improvement has been achieved by the additional chlorine emissions, with NMB
585 decreasing from -96% – -79% to -36% – 39% for Cl simulation. The comparison with observed N₂O₅
586 and ClNO₂ also indicates better model performance with Yu parameterization while $\gamma_{\text{N}_2\text{O}_5}$ and ϕ_{ClNO_2} are
587 underestimated in McDuffie parameterization (a default setting in GEOS-Chem), resulting in larger
588 model bias. The simulation of O₃ and PM_{2.5} also agrees better with observations in general in the Base
589 case (with the additional chlorine emissions and Yu parameterization) than the others.

590 Total tropospheric chlorine chemistry could increase Cl atoms by up to 7×10^3 molec cm⁻³, and leads to
591 an increase of up to 4.5 ppbv in MDA8 O₃ but a decrease of up to 7.9 $\mu\text{g m}^{-3}$ in PM_{2.5} concentrations on
592 an annual mean basis in China. The decrease in PM_{2.5} is mainly associated with the decrease in NO₃⁻ and
593 NH₄⁺, by up to 6.4 and 1.9 $\mu\text{g m}^{-3}$, respectively. The results also indicate that the heterogeneous N₂O₅ +
594 Cl chemistry dominate the impact of chlorine chemistry, accounting for 83% and 90% of total change in
595 O₃ and PM_{2.5} concentrations. In other words, the chlorine chemistry without the heterogeneous N₂O₅ +
596 Cl chemistry has a minor effect on annual mean MDA8 O₃ (less than 0.7 ppbv) and PM_{2.5} (less than 1.5
597 $\mu\text{g m}^{-3}$) concentrations in China. This mechanism is particularly useful in elucidating the commonly seen
598 O₃ underestimations relative to observations (e.g. (Ma et al. (2019))).

599 The effect of the heterogeneous N₂O₅ + Cl chemistry is sensitive to chlorine emissions. With the
600 additional anthropogenic and biomass burning sources, simulated PM_{2.5} concentrations are increased by
601 up to 4.5 $\mu\text{g m}^{-3}$ in the North China Plain but decreased by up to 3.7 $\mu\text{g m}^{-3}$ in the Sichuan Basin on an
602 annual basis. The latter is mainly driven by the decrease of NO₃⁻ due to the competition between the
603 formation of ClNO₂ and HNO₃ upon the uptake of N₂O₅ on aerosol surfaces. The additional emissions
604 also increase Cl atoms and OH in China associated with the photolysis of ClNO₂, consequently leading

605 to an increase of annual mean MDA8 O₃ concentrations by up to 3.5 ppbv. In contrast, the significance
606 of the heterogeneous N₂O₅ + Cl chemistry especially over inland China would be severely
607 underestimated if only sea salt chlorine is considered, with only a slight increase in MDA8 O₃ (< 0.5
608 ppbv) and a minor decrease in PM_{2.5} (< 1.5 μg m⁻³) in inland China.

609 Moreover, we found the importance of chlorine chemistry not only depends on the amount of emissions,
610 but is also sensitive to the parameterizations for the heterogeneous N₂O₅ + Cl chemistry. Although with
611 the same emission, the effects on MDA8 O₃ and PM_{2.5} in China from the McDuffie case are lower
612 compared to the results with Yu parameterization: differing by 48% and 27% in the annual average,
613 respectively.

614 **Acknowledgements**

615 This study is supported by the National key R&D Program of China (2018YFC0213901), the National
616 Natural Science Foundation of China (41907182, 41877303, 91644218, 41877302, 41875156), the
617 Fundamental Research Funds for the Central Universities (21621105), Guangdong Natural Science
618 Funds for Distinguished Young Scholar (grant No. 2018B030306037), the Guangdong Innovative and
619 Entrepreneurial Research Team Program (Research team on atmospheric environmental roles and
620 effects of carbonaceous species: 2016ZT06N263), and Special Fund Project for Science and
621 Technology Innovation Strategy of Guangdong Province (2019B121205004).

622 **Competing interests.**

623 The authors declare that they have no conflict of interest.

624 **Data and Code availability**

625 The data used in this study is available upon request from Qiaoqiao Wang (qwang@jnu.edu.cn). The
626 revised codes for different simulations could be downloaded via
627 <https://zenodo.org/record/5957287#.YfyNMppBxPZ>

628 **References**

- 629 Anttila, T., Kiendler-Scharr, A., Tillmann, R., and Mentel, T. F.: On the Reactive Uptake of Gaseous
630 Compounds by Organic-Coated Aqueous Aerosols: Theoretical Analysis and Application to the
631 Heterogeneous Hydrolysis of N₂O₅, *The Journal of Physical Chemistry A*, 110, 10435-10443,
632 10.1021/jp062403c, 2006.
- 633 Atkinson, R., Baulch, D. L., Cox, R. A., Crowley, J. N., Hampson, R. F., Hynes, R. G., Jenkin, M. E.,
634 Rossi, M. J., Troe, J., and Subcommittee, I.: Evaluated kinetic and photochemical data for
635 atmospheric chemistry: Volume II - gas phase reactions of organic species, *Atmos. Chem. Phys.*, 6,
636 3625-4055, 10.5194/acp-6-3625-2006, 2006.
- 637 Bertram, T. H. and Thornton, J. A.: Toward a general parameterization of N₂O₅ reactivity on aqueous
638 particles: the competing effects of particle liquid water, nitrate and chloride, *Atmospheric Chemistry
639 & Physics Discussions*, 9, 191-198, 2009.
- 640 Bertram, T. H., Perring, A. E., Wooldridge, P. J., Dibb, J., Avery, M. A., and Cohen, R. C.: On the export
641 of reactive nitrogen from Asia: NO_x partitioning and effects on ozone, *Atmos. Chem. Phys.*, 13,
642 4617-4630, 10.5194/acp-13-4617-2013, 2013.
- 643 Chang, W. L., Brown, S. S., Stutz, J., Middlebrook, A. M., Bahreini, R., Wagner, N. L., Dubé, W. P.,
644 Pollack, I. B., Ryerson, T. B., and Riemer, N.: Evaluating N₂O₅ heterogeneous hydrolysis
645 parameterizations for CalNex 2010, *J. Geophys. Res.: Atmos.*, 121, 5051-5070,
646 <https://doi.org/10.1002/2015JD024737>, 2016.
- 647 Chen, C., Zhang, H., Yan, W., Wu, N., Zhang, Q., and He, K.: Aerosol water content enhancement leads
648 to changes in the major formation mechanisms of nitrate and secondary organic aerosols in winter
649 over the North China Plain, *Environ. Pollut.*, 287, 117625,
650 <https://doi.org/10.1016/j.envpol.2021.117625>, 2021a.
- 651 Chen, W., Ye, Y., Hu, W., Zhou, H., Pan, T., Wang, Y., Song, W., Song, Q., Ye, C., Wang, C., Wang, B.,
652 Huang, S., Yuan, B., Zhu, M., Lian, X., Zhang, G., Bi, X., Jiang, F., Liu, J., Canonaco, F., Prevot,
653 A. S. H., Shao, M., and Wang, X.: Real-Time Characterization of Aerosol Compositions, Sources,
654 and Aging Processes in Guangzhou During PRIDE-GBA 2018 Campaign, *J. Geophys. Res.: Atmos.*,
655 126, e2021JD035114, <https://doi.org/10.1029/2021JD035114>, 2021b.
- 656 Choi, M. S., Qiu, X., Zhang, J., Wang, S., Li, X., Sun, Y., Chen, J., and Ying, Q.: Study of Secondary
657 Organic Aerosol Formation from Chlorine Radical-Initiated Oxidation of Volatile Organic
658 Compounds in a Polluted Atmosphere Using a 3D Chemical Transport Model, *Environ. Sci.
659 Technol.*, 54, 13409-13418, 10.1021/acs.est.0c02958, 2020.

660 Dai, J., Liu, Y., Wang, P., Fu, X., Xia, M., and Wang, T.: The impact of sea-salt chloride on ozone through
661 heterogeneous reaction with N₂O₅ in a coastal region of south China, *Atmos. Environ.*, 236, 117604,
662 <https://doi.org/10.1016/j.atmosenv.2020.117604>, 2020.

663 DeCarlo, P. F., Kimmel, J. R., Trimborn, A., Northway, M. J., Jayne, J. T., Aiken, A. C., Gonin, M., Fuhrer,
664 K., Horvath, T., Docherty, K. S., Worsnop, D. R., and Jimenez, J. L.: Field-Deployable, High-
665 Resolution, Time-of-Flight Aerosol Mass Spectrometer, *Anal. Chem.*, 78, 8281-8289,
666 10.1021/ac061249n, 2006.

667 Finlayson-Pitts, B. J., Ezell, M. J., and Pitts, J. N. J.: Formation of chemically active chlorine compounds
668 by reactions of atmospheric NaCl particles with gaseous N₂O₅ and ClONO₂, *Cheminform*, 20, 241-
669 244, 1989.

670 Fountoukis, C. and Nenes, A.: ISORROPIA II: a computationally efficient thermodynamic equilibrium
671 model for K⁺-Ca²⁺-Mg²⁺-NH₄⁺-Na⁺-SO₄²⁻-NO₃⁻-Cl⁻-H₂O aerosols, *Atmos. Chem. Phys.*, 7, 4639-
672 4659, 10.5194/acp-7-4639-2007, 2007.

673 Fu, X., Wang, T., Wang, S., Zhang, L., Cai, S., Xing, J., and Hao, J.: Anthropogenic Emissions of
674 Hydrogen Chloride and Fine Particulate Chloride in China, *Environ. Sci. Technol.*, 52, 1644, 2018.

675 Geng, G., Zhang, Q., Martin, R. V., Van Donkelaar, A., Huo, H., Che, H., Lin, J., and He, K.: Estimating
676 long-term PM_{2.5} concentrations in China using satellite-based aerosol optical depth and a chemical
677 transport model, *Remote Sens. Environ.*, 166, 262-270, 2015.

678 Griffiths, P. T., Badger, C. L., Cox, R. A., Folkers, M., Henk, H. H., and Mentel, T. F.: Reactive Uptake
679 of N₂O₅ by Aerosols Containing Dicarboxylic Acids. Effect of Particle Phase, Composition, and
680 Nitrate Content, *The Journal of Physical Chemistry A*, 113, 5082-5090, 10.1021/jp8096814, 2009.

681 Gross, S., Iannone, R., Xiao, S., and Bertram, A. K.: Reactive uptake studies of NO₃ and N₂O₅ on
682 alkenoic acid, alkanoate, and polyalcohol substrates to probe nighttime aerosol chemistry, *PCCP*,
683 11, 7792-7803, 10.1039/B904741G, 2009.

684 Guenther, A., Karl, T., Harley, P., Wiedinmyer, C., Palmer, P. I., and Geron, C.: Estimates of global
685 terrestrial isoprene emissions using MEGAN (Model of Emissions of Gases and Aerosols from
686 Nature), *Atmos. Chem. Phys.*, 6, 3181-3210, 10.5194/acp-6-3181-2006, 2006.

687 Haskins, J. D., Lee, B. H., Lopez-Hilifiker, F. D., Peng, Q., Jaeglé, L., Reeves, J. M., Schroder, J. C.,
688 Campuzano-Jost, P., Fibiger, D., McDuffie, E. E., Jiménez, J. L., Brown, S. S., and Thornton, J. A.:
689 Observational Constraints on the Formation of Cl₂ From the Reactive Uptake of ClONO₂ on Aerosols
690 in the Polluted Marine Boundary Layer, *J. Geophys. Res.: Atmos.*, 124, 8851-8869,
691 <https://doi.org/10.1029/2019JD030627>, 2019.

692 Hong, Y., Liu, Y., Chen, X., Fan, Q., Chen, C., Chen, X., and Wang, M.: The role of anthropogenic

693 chlorine emission in surface ozone formation during different seasons over eastern China, *Sci. Total*
694 *Environ.*, 723, 137697, <https://doi.org/10.1016/j.scitotenv.2020.137697>, 2020.

695 Hossaini, R., Chipperfield, M. P., Saiz-Lopez, A., Fernandez, R., Monks, S., Feng, W., Brauer, P., and
696 von Glasow, R.: A global model of tropospheric chlorine chemistry: Organic versus inorganic
697 sources and impact on methane oxidation, *J. Geophys. Res.: Atmos.*, 121, 14,271-214,297,
698 <https://doi.org/10.1002/2016JD025756>, 2016.

699 Huang, Z., Zhong, Z., Sha, Q., Xu, Y., Zhang, Z., Wu, L., Wang, Y., Zhang, L., Cui, X., Tang, M., Shi,
700 B., Zheng, C., Li, Z., Hu, M., Bi, L., Zheng, J., and Yan, M.: An updated model-ready emission
701 inventory for Guangdong Province by incorporating big data and mapping onto multiple chemical
702 mechanisms, *Sci. Total Environ.*, 769, 144535, <https://doi.org/10.1016/j.scitotenv.2020.144535>,
703 2021.

704 Jaeglé, L., Quinn, P. K., Bates, T. S., Alexander, B., and Lin, J. T.: Global distribution of sea salt aerosols:
705 new constraints from in situ and remote sensing observations, *Atmos. Chem. Phys.*, 11, 3137-3157,
706 10.5194/acp-11-3137-2011, 2011.

707 Kercher, J. P., Riedel, T. P., and Thornton, J. A.: Chlorine activation by N₂O₅: simultaneous, in situ
708 detection of ClNO₂ and N₂O₅ by chemical ionization mass spectrometry, *Atmospheric*
709 *Measurement Techniques Discussions*, 2009.

710 Lawler, M. J., Sander, R., Carpenter, L. J., Lee, J. D., and Saltzman, E. S.: HOCl and Cl₂ observations
711 in marine air, *Atmos. Chem. Phys.*, 11, 8115-8144, 10.5194/acp-11-7617-2011, 2011.

712 Le Breton, M., Hallquist, Å. M., Pathak, R. K., Simpson, D., Wang, Y., Johansson, J., Zheng, J., Yang,
713 Y., Shang, D., Wang, H., Liu, Q., Chan, C., Wang, T., Bannan, T. J., Priestley, M., Percival, C. J.,
714 Shallcross, D. E., Lu, K., Guo, S., Hu, M., and Hallquist, M.: Chlorine oxidation of VOCs at a semi-
715 rural site in Beijing: Significant chlorine liberation from ClNO₂ and subsequent gas and particle
716 phase Cl-VOC production, *Atmos. Chem. Phys.*, 18, 13013-13030, 10.5194/acp-18-13013-2018,
717 2018.

718 Li, G., Su, H., Ma, N., Tao, J., Kuang, Y., Wang, Q., Hong, J., Zhang, Y., Kuhn, U., Zhang, S., Pan, X.,
719 Lu, N., Tang, M., Zheng, G., Wang, Z., Gao, Y., Cheng, P., Xu, W., Zhou, G., Zhao, C., Yuan, B.,
720 Shao, M., Ding, A., Zhang, Q., Fu, P., Sun, Y., Pöschl, U., and Cheng, Y.: Multiphase chemistry
721 experiment in Fogs and Aerosols in the North China Plain (McFAN): integrated analysis and
722 intensive winter campaign 2018, *Faraday Discuss.*, 226, 207-222, 10.1039/D0FD00099J, 2021.

723 Li, K., Jacob, D. J., Liao, H., Shen, L., Zhang, Q., and Bates, K. H.: Anthropogenic drivers of 2013–2017
724 trends in summer surface ozone in China, *P. Natl. Acad. Sci.*, 116, 422-427,
725 10.1073/pnas.1812168116, 2019.

726 Li, M., Zhang, Q., Kurokawa, J. I., Woo, J. H., He, K., Lu, Z., Ohara, T., Song, Y., Streets, D. G.,
727 Carmichael, G. R., Cheng, Y., Hong, C., Huo, H., Jiang, X., Kang, S., Liu, F., Su, H., and Zheng,
728 B.: MIX: a mosaic Asian anthropogenic emission inventory under the international collaboration
729 framework of the MICS-Asia and HTAP, *Atmos. Chem. Phys.*, 17, 935-963, 10.5194/acp-17-935-
730 2017, 2017.

731 Li, Q., Zhang, L., Wang, T., Tham, Y. J., Ahmadov, R., Xue, L., Zhang, Q., and Zheng, J.: Impacts of
732 heterogeneous uptake of dinitrogen pentoxide and chlorine activation on ozone and reactive
733 nitrogen partitioning: improvement and application of the WRF-Chem model in southern China,
734 *Atmos. Chem. Phys.*, 16, 14875-14890, 10.5194/acp-16-14875-2016, 2016.

735 Liu, X., Qu, H., Huey, L. G., Wang, Y., Sjostedt, S., Zeng, L., Lu, K., Wu, Y., Hu, M., Shao, M., Zhu, T.,
736 and Zhang, Y.: High Levels of Daytime Molecular Chlorine and Nitryl Chloride at a Rural Site on
737 the North China Plain, *Environ. Sci. Technol.*, 51, 9588-9595, 10.1021/acs.est.7b03039, 2017.

738 Liu, Y., Fan, Q., Chen, X., Zhao, J., Ling, Z., Hong, Y., Li, W., Chen, X., Wang, M., and Wei, X.:
739 Modeling the impact of chlorine emissions from coal combustion and prescribed waste incineration
740 on tropospheric ozone formation in China, *Atmos. Chem. Phys.*, 18, 2709-2724, 10.5194/acp-18-
741 2709-2018, 2018.

742 Lobert, J. M., Keene, W. C., Logan, J. A., and Yevich, R.: Global chlorine emissions from biomass
743 burning: Reactive Chlorine Emissions Inventory, *J. Geophys. Res.: Atmos.*, 104, 8373-8389,
744 <https://doi.org/10.1029/1998JD100077>, 1999.

745 Ma, M., Gao, Y., Wang, Y., Zhang, S., Leung, L. R., Liu, C., Wang, S., Zhao, B., Chang, X., Su, H.,
746 Zhang, T., Sheng, L., Yao, X., and Gao, H.: Substantial ozone enhancement over the North China
747 Plain from increased biogenic emissions due to heat waves and land cover in summer 2017, *Atmos.*
748 *Chem. Phys.*, 19, 12195-12207, 10.5194/acp-19-12195-2019, 2019.

749 McDuffie, E. E., Fibiger, D. L., Dubé, W. P., Lopez-Hilfiker, F., Lee, B. H., Jaeglé, L., Guo, H., Weber,
750 R. J., Reeves, J. M., Weinheimer, A. J., Schroder, J. C., Campuzano-Jost, P., Jimenez, J. L., Dibb, J.
751 E., Veres, P., Ebben, C., Sparks, T. L., Wooldridge, P. J., Cohen, R. C., Campos, T., Hall, S. R.,
752 Ullmann, K., Roberts, J. M., Thornton, J. A., and Brown, S. S.: CINO₂ Yields From Aircraft
753 Measurements During the 2015 WINTER Campaign and Critical Evaluation of the Current
754 Parameterization, *J. Geophys. Res.: Atmos.*, 123, 12,994-913,015,
755 <https://doi.org/10.1029/2018JD029358>, 2018a.

756 McDuffie, E. E., Fibiger, D. L., Dubé, W. P., Lopez-Hilfiker, F., Lee, B. H., Thornton, J. A., Shah, V.,
757 Jaeglé, L., Guo, H., Weber, R. J., Michael Reeves, J., Weinheimer, A. J., Schroder, J. C.,
758 Campuzano-Jost, P., Jimenez, J. L., Dibb, J. E., Veres, P., Ebben, C., Sparks, T. L., Wooldridge, P.
759 J., Cohen, R. C., Hornbrook, R. S., Apel, E. C., Campos, T., Hall, S. R., Ullmann, K., and Brown,

760 S. S.: Heterogeneous N₂O₅ Uptake During Winter: Aircraft Measurements During the 2015
761 WINTER Campaign and Critical Evaluation of Current Parameterizations, *J. Geophys. Res.: Atmos.*,
762 123, 4345-4372, <https://doi.org/10.1002/2018JD028336>, 2018b.

763 Mitroo, D., Gill, T. E., Haas, S., Pratt, K. A., and Gaston, C. J.: ClNO₂ Production from N₂O₅ Uptake
764 on Saline Playa Dusts: New Insights into Potential Inland Sources of ClNO₂, *Environ. Sci. Technol.*,
765 53, 7442-7452, 2019.

766 Morgan, W. T., Ouyang, B., Allan, J. D., Aruffo, E., Di Carlo, P., Kennedy, O. J., Lowe, D., Flynn, M. J.,
767 Rosenberg, P. D., Williams, P. I., Jones, R., McFiggans, G. B., and Coe, H.: Influence of aerosol
768 chemical composition on N₂O₅ uptake: airborne regional measurements in northwestern Europe,
769 *Atmos. Chem. Phys.*, 15, 973-990, [10.5194/acp-15-973-2015](https://doi.org/10.5194/acp-15-973-2015), 2015.

770 Ng, N. L., Herndon, S. C., Trimborn, A., Canagaratna, M. R., Croteau, P. L., Onasch, T. B., Sueper, D.,
771 Worsnop, D. R., Zhang, Q., Sun, Y. L., and Jayne, J. T.: An Aerosol Chemical Speciation Monitor
772 (ACSM) for Routine Monitoring of the Composition and Mass Concentrations of Ambient Aerosol,
773 *Aerosol Sci. Technol.*, 45, 780-794, [10.1080/02786826.2011.560211](https://doi.org/10.1080/02786826.2011.560211), 2011.

774 Osthoff, H. D., Roberts, J. M., Ravishankara, A. R., Williams, E. J., Lerner, B. M., Sommariva, R., Bates,
775 T. S., Coffman, D., Quinn, P. K., Dibb, J. E., Stark, H., Burkholder, J. B., Talukdar, R. K., Meagher,
776 J., Fehsenfeld, F. C., and Brown, S. S.: High levels of nitryl chloride in the polluted subtropical
777 marine boundary layer, *Nat. Geosci.*, 1, 324-328, [10.1038/ngeo177](https://doi.org/10.1038/ngeo177), 2008.

778 Riedel, T. P., Bertram, T. H., Crisp, T. A., Williams, E. J., Lerner, B. M., Vlasenko, A., Li, S. M., Gilman,
779 J., De Gouw, J., and Bon, D. M.: Nitryl Chloride and Molecular Chlorine in the Coastal Marine
780 Boundary Layer, *Environ. Sci. Technol.*, 46, 10463-10470, 2012.

781 Riemer, N., Vogel, H., Vogel, B., Anttila, T., Kiendler-Scharr, A., and Mentel, T. F.: Relative importance
782 of organic coatings for the heterogeneous hydrolysis of N₂O₅ during summer in Europe, *J. Geophys.*
783 *Res.: Atmos.*, 114, <https://doi.org/10.1029/2008JD011369>, 2009.

784 Saiz-Lopez, A. and von Glasow, R.: Reactive halogen chemistry in the troposphere, *Chem. Soc. Rev.*, 41,
785 6448-6472, [10.1039/C2CS35208G](https://doi.org/10.1039/C2CS35208G), 2012.

786 Sarwar, G., Simon, H., Xing, J., and Mathur, R.: Importance of tropospheric ClNO₂ chemistry across the
787 Northern Hemisphere, *Geophys. Res. Lett.*, 2014.

788 Schmidt, J. A., Jacob, D. J., Horowitz, H. M., Hu, L., Sherwen, T., Evans, M. J., Liang, Q., Suleiman, R.
789 M., Oram, D. E., Le Breton, M., Percival, C. J., Wang, S., Dix, B., and Volkamer, R.: Modeling the
790 observed tropospheric BrO background: Importance of multiphase chemistry and implications for
791 ozone, OH, and mercury, *J. Geophys. Res.: Atmos.*, 121, 8118-8118, <https://doi.org/10.1002/2015JD024229>, 2016.

793 Sherwen, T., Evans, M. J., Sommariva, R., Hollis, L. D. J., Ball, S. M., Monks, P. S., Reed, C., Carpenter,
794 L. J., Lee, J. D., Forster, G., Bandy, B., Reeves, C. E., and Bloss, W. J.: Effects of halogens on
795 European air-quality, *Faraday Discuss.*, 200, 75-100, 10.1039/C7FD00026J, 2017.

796 Sherwen, T., Schmidt, J. A., Evans, M. J., Carpenter, L. J., Großmann, K., Eastham, S. D., Jacob, D. J.,
797 Dix, B., Koenig, T. K., Sinreich, R., Ortega, I., Volkamer, R., Saiz-Lopez, A., Prados-Roman, C.,
798 Mahajan, A. S., and Ordóñez, C.: Global impacts of tropospheric halogens (Cl, Br, I) on oxidants
799 and composition in GEOS-Chem, *Atmos. Chem. Phys.*, 16, 12239-12271, 10.5194/acp-16-12239-
800 2016, 2016.

801 Simmonds, P. G., Manning, A. J., Cunnold, D. M., McCulloch, A., O'Doherty, S., Derwent, R. G.,
802 Krummel, P. B., Fraser, P. J., Dunse, B., Porter, L. W., Wang, R. H. J., Grealley, B. R., Miller, B. R.,
803 Salameh, P., Weiss, R. F., and Prinn, R. G.: Global trends, seasonal cycles, and European emissions
804 of dichloromethane, trichloroethene, and tetrachloroethene from the AGAGE observations at Mace
805 Head, Ireland, and Cape Grim, Tasmania, *J. Geophys. Res.: Atmos.*, 111,
806 <https://doi.org/10.1029/2006JD007082>, 2006.

807 Simpson, W. R., Brown, S. S., Saiz-Lopez, A., Thornton, J. A., and von Glasow, R.: Tropospheric
808 Halogen Chemistry: Sources, Cycling, and Impacts, *Chem. Rev.*, 115, 4035-4062,
809 10.1021/cr5006638, 2015.

810 Staudt, S., Gord, J. R., Karimova, N. V., McDuffie, E. E., Brown, S. S., Gerber, R. B., Nathanson, G. M.,
811 and Bertram, T. H.: Sulfate and Carboxylate Suppress the Formation of ClNO₂ at Atmospheric
812 Interfaces, *ACS Earth and Space Chemistry*, 3, 1987-1997, 10.1021/acsearthspacechem.9b00177,
813 2019.

814 Thornton, J. A., Braban, C. F., and Abbatt, J. P. D.: N₂O₅ hydrolysis on sub-micron organic aerosols: the
815 effect of relative humidity, particle phase, and particle size, *PCCP*, 5, 4593-4603, 10.1039/B307498F,
816 2003.

817 Tian, M., Liu, Y., Yang, F., Zhang, L., Peng, C., Chen, Y., Shi, G., Wang, H., Luo, B., Jiang, C., Li, B.,
818 Takeda, N., and Koizumi, K.: Increasing importance of nitrate formation for heavy aerosol pollution
819 in two megacities in Sichuan Basin, southwest China, *Environ. Pollut.*, 250, 898-905,
820 <https://doi.org/10.1016/j.envpol.2019.04.098>, 2019.

821 Van, d. W., G. R., Randerson, J. T., Giglio, L., Collatz, G. J., Mu, M., Kasibhatla, P. S., Morton, D. C.,
822 Defries, R. S., Jin, Y., and Van Leeuwen, T. T.: Global fire emissions and the contribution of
823 deforestation, savanna, forest, agricultural, and peat fires (1997–2009), *Atmos. Chem. Phys.*, 10,
824 16153-16230, 10.5194/acp-10-11707-2010, 2010.

825 Wang, S., Su, H., Chen, C., Tao, W., Streets, D. G., Lu, Z., Zheng, B., Carmichael, G. R., Lelieveld, J.,
826 Pöschl, U., and Cheng, Y.: Natural gas shortages during the “coal-to-gas” transition in China have

827 caused a large redistribution of air pollution in winter 2017, *P. Natl. Acad. Sci.*, 117, 31018-31025,
828 10.1073/pnas.2007513117, 2020a.

829 Wang, X., Jacob, D. J., Fu, X., Wang, T., and Liao, H.: Effects of Anthropogenic Chlorine on PM 2.5 and
830 Ozone Air Quality in China, *Environ. Sci. Technol.*, 54, 9908-9916, 2020b.

831 Wang, X., Jacob, D. J., Eastham, S. D., Sulprizio, M. P., Zhu, L., Chen, Q., Alexander, B., Sherwen, T.,
832 Evans, M. J., Lee, B. H., Haskins, J. D., Lopez-Hilfiker, F. D., Thornton, J. A., Huey, G. L., and
833 Liao, H.: The role of chlorine in global tropospheric chemistry, *Atmos. Chem. Phys.*, 19, 3981-4003,
834 10.5194/acp-19-3981-2019, 2019.

835 Wang, Y., Shen, L., Wu, S., Mickley, L., He, J., and Hao, J.: Sensitivity of surface ozone over China to
836 2000–2050 global changes of climate and emissions, *Atmos. Environ.*, 75, 374-382, 2013.

837 Xia, M., Wang, W., Wang, Z., Gao, J., Li, H., Liang, Y., Yu, C., Zhang, Y., Wang, P., Zhang, Y., Bi, F.,
838 Cheng, X., and Wang, T.: Heterogeneous Uptake of N₂O₅ in Sand Dust and Urban Aerosols
839 Observed during the Dry Season in Beijing, *Atmosphere*, 10, 204, 2019.

840 Xu, Z., Liu, M., Zhang, M., Song, Y., Wang, S., Zhang, L., Xu, T., Wang, T., Yan, C., Zhou, T., Sun, Y.,
841 Pan, Y., Hu, M., Zheng, M., and Zhu, T.: High efficiency of livestock ammonia emission controls
842 in alleviating particulate nitrate during a severe winter haze episode in northern China, *Atmos. Chem.*
843 *Phys.*, 19, 5605-5613, 10.5194/acp-19-5605-2019, 2019.

844 Yang, X., Wang, T., Xia, M., Gao, X., Li, Q., Zhang, N., Gao, Y., Lee, S., Wang, X., Xue, L., Yang, L.,
845 and Wang, W.: Abundance and origin of fine particulate chloride in continental China, *Sci. Total*
846 *Environ.*, 624, 1041-1051, <https://doi.org/10.1016/j.scitotenv.2017.12.205>, 2018.

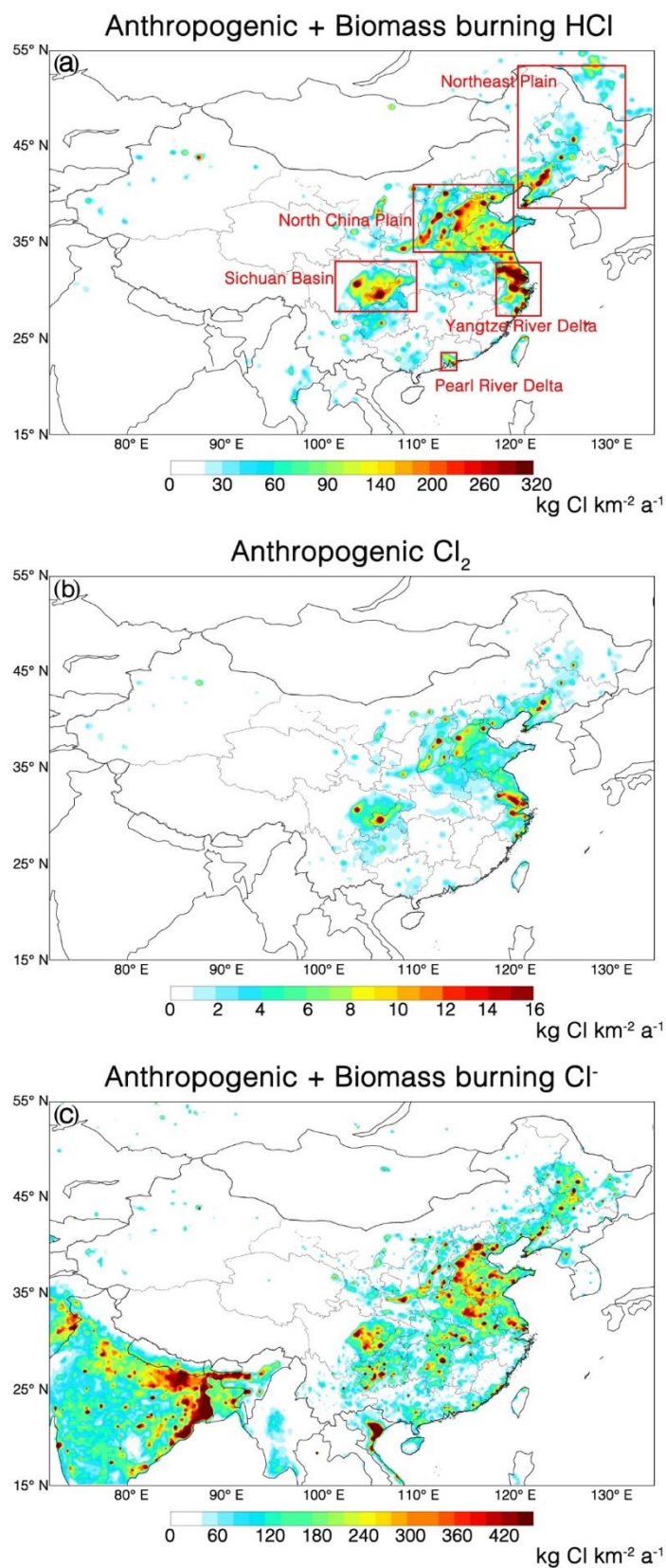
847 Ye, C., Yuan, B., Lin, Y., Wang, Z., Hu, W., Li, T., Chen, W., Wu, C., Wang, C., Huang, S., Qi, J., Wang,
848 B., Wang, C., Song, W., Wang, X., Zheng, E., Krechmer, J. E., Ye, P., Zhang, Z., Wang, X., Worsnop,
849 D. R., and Shao, M.: Chemical characterization of oxygenated organic compounds in the gas phase
850 and particle phase using iodide CIMS with FIGAERO in urban air, *Atmos. Chem. Phys.*, 21, 8455-
851 8478, 10.5194/acp-21-8455-2021, 2021.

852 Yu, C., Wang, Z., Xia, M., Fu, X., Wang, W., Tham, Y. J., Chen, T., Zheng, P., Li, H., Shan, Y., Wang, X.,
853 Xue, L., Zhou, Y., Yue, D., Ou, Y., Gao, J., Lu, K., Brown, S. S., Zhang, Y., and Wang, T.:
854 Heterogeneous N₂O₅ reactions on atmospheric aerosols at four Chinese sites: improving model
855 representation of uptake parameters, *Atmos. Chem. Phys.*, 20, 4367-4378, 10.5194/acp-20-4367-
856 2020, 2020.

857 Zhang, T., de Jong, M. C., Wooster, M. J., Xu, W., and Wang, L.: Trends in eastern China agricultural
858 fire emissions derived from a combination of geostationary (Himawari) and polar (VIIRS) orbiter
859 fire radiative power products, *Atmos. Chem. Phys.*, 20, 10687-10705, 10.5194/acp-20-10687-2020,

860 2020.

861

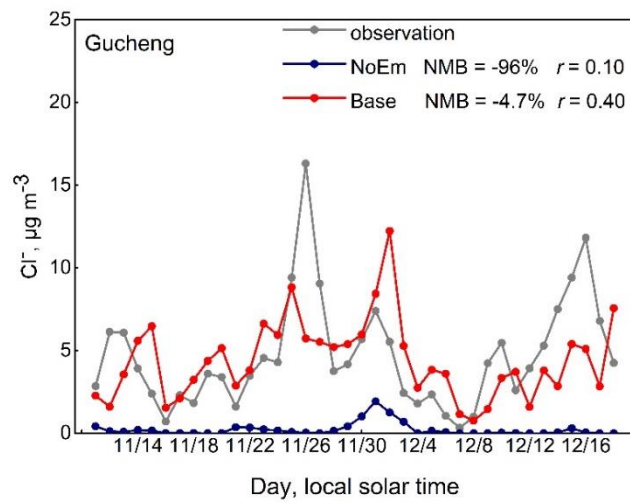
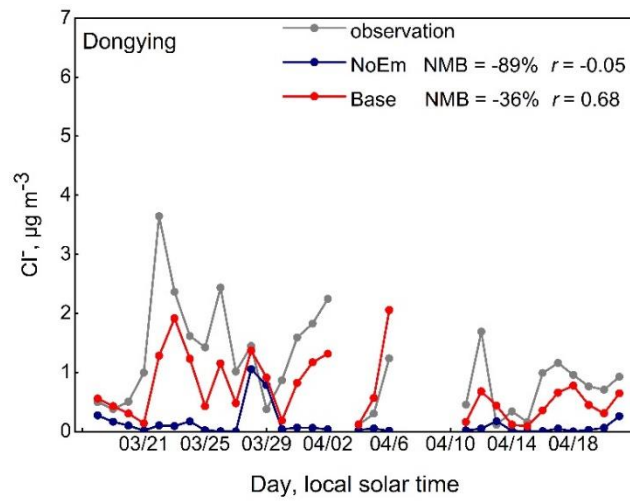
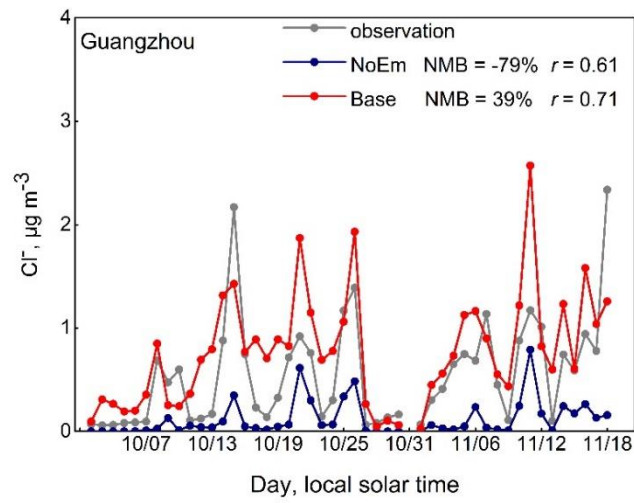


862
863

Figure 1. Annual emissions of (a) HCl, (b) Cl₂, (c) non-sea salt Cl⁻. Locations of the Northeast Plain, North

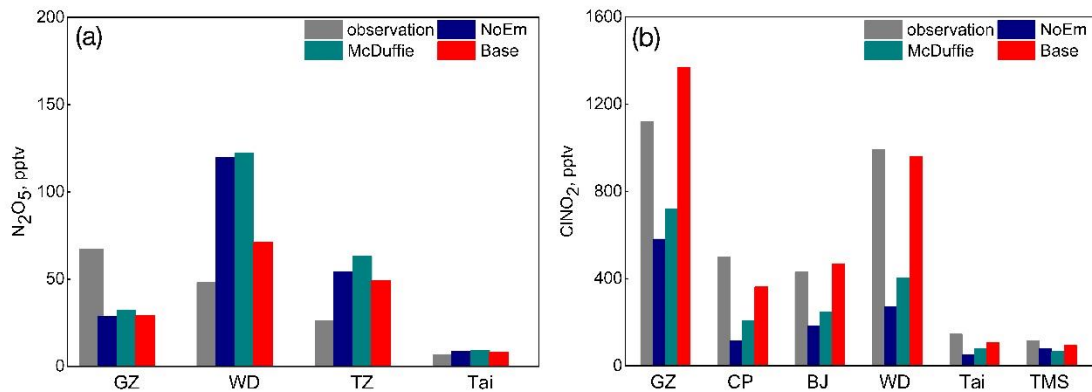
864
865

China Plain, Yangtze River Delta, Pearl River Delta and Sichuan Basin are highlighted by red boxes in (a).

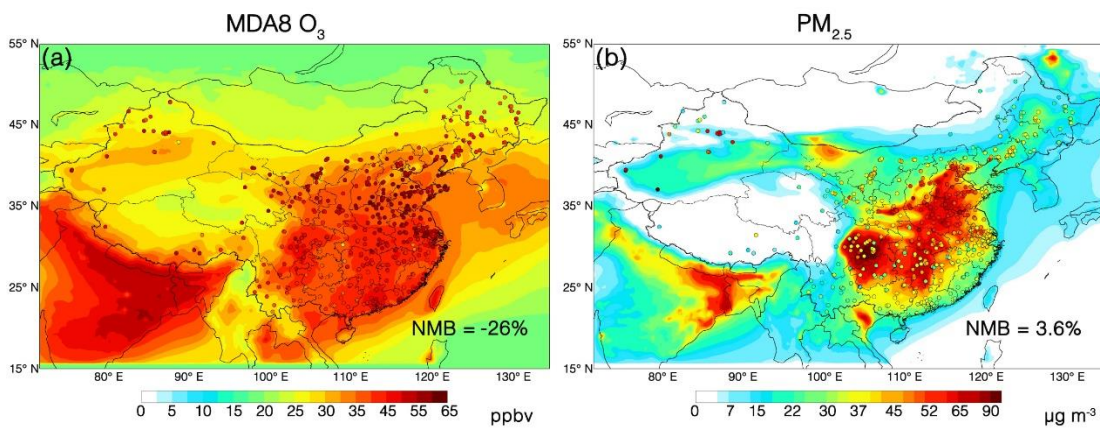


866

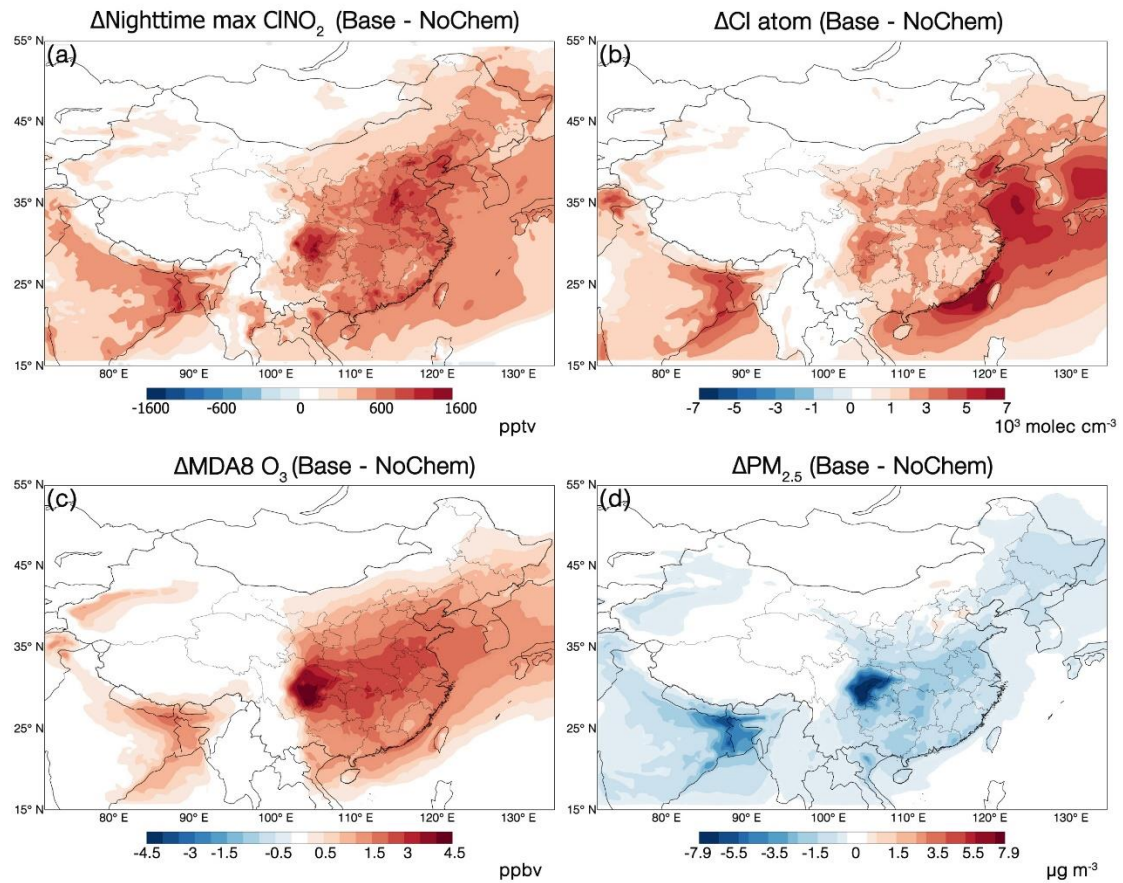
867 **Figure 2. Time series of simulated and observed particulate Cl^- concentrations at the Guangzhou, Dongying**
 868 **and Gucheng sites.**
 869



870
 871 **Figure 3. Comparison of observed and simulated (a) averaged N_2O_5 concentrations and (b) mean nighttime**
 872 **maximum mixing ratio of $ClNO_2$ concentrations at different sites. The simulation definitions are provided in**
 873 **Table 2. GZ: Guangzhou; WD: Wangdu; TZ: Taizhou; Tai: Mount Tai; CP: Changping; BJ: Beijing; TMS:**
 874 **Mount TaiMoShan**
 875



876
 877 **Figure 4. Annual mean surface concentrations of (a) MDA8 O_3 and (b) $PM_{2.5}$ over China in 2018. GEOS-**
 878 **Chem model values from the Base case are shown as contours. Observations from China National**
 879 **Environmental Monitoring Center (CNEMC) are shown as circles.**
 880



881

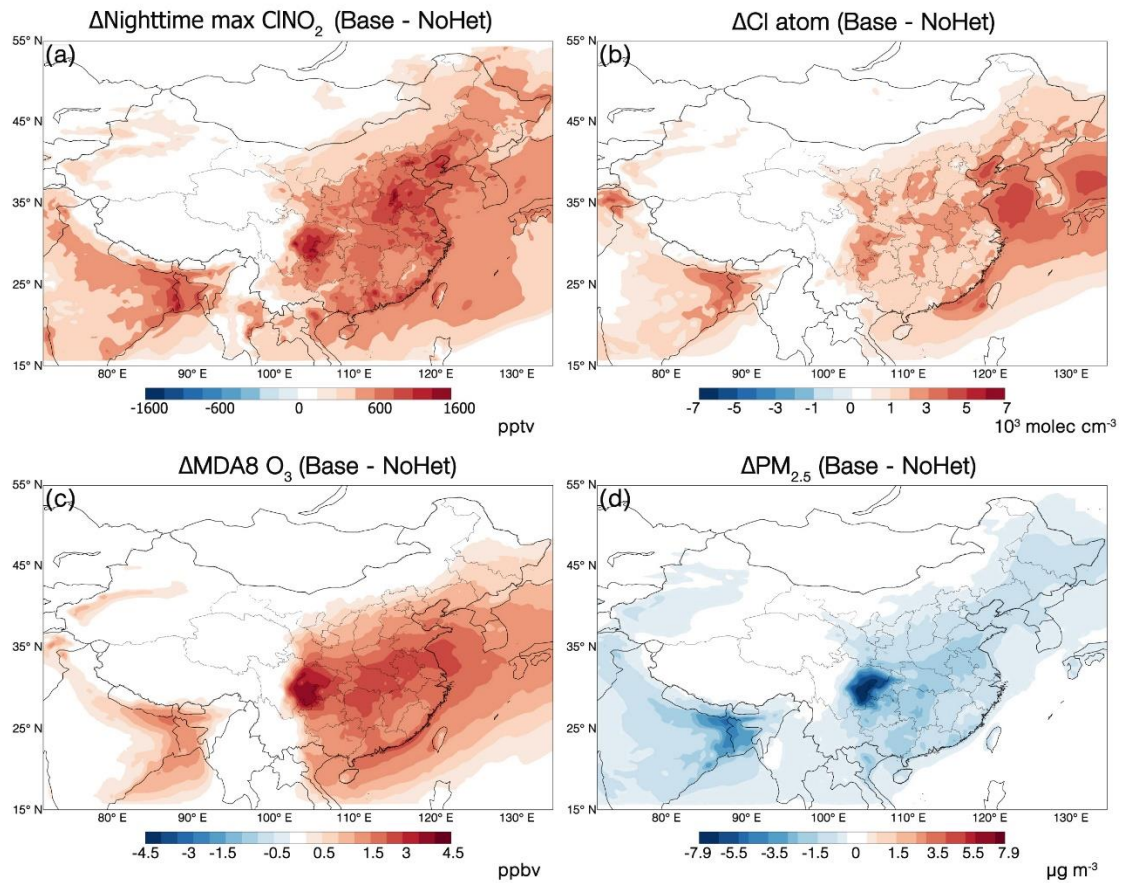
882 **Figure 5. Effects of chlorine chemistry on annual mean surface concentrations of (a) nighttime max ClNO_2 ,**

883 **(b) Cl atom, (c) MDA8 O_3 and (d) PM_{2.5} in China, estimated as the differences between the Base and**

884

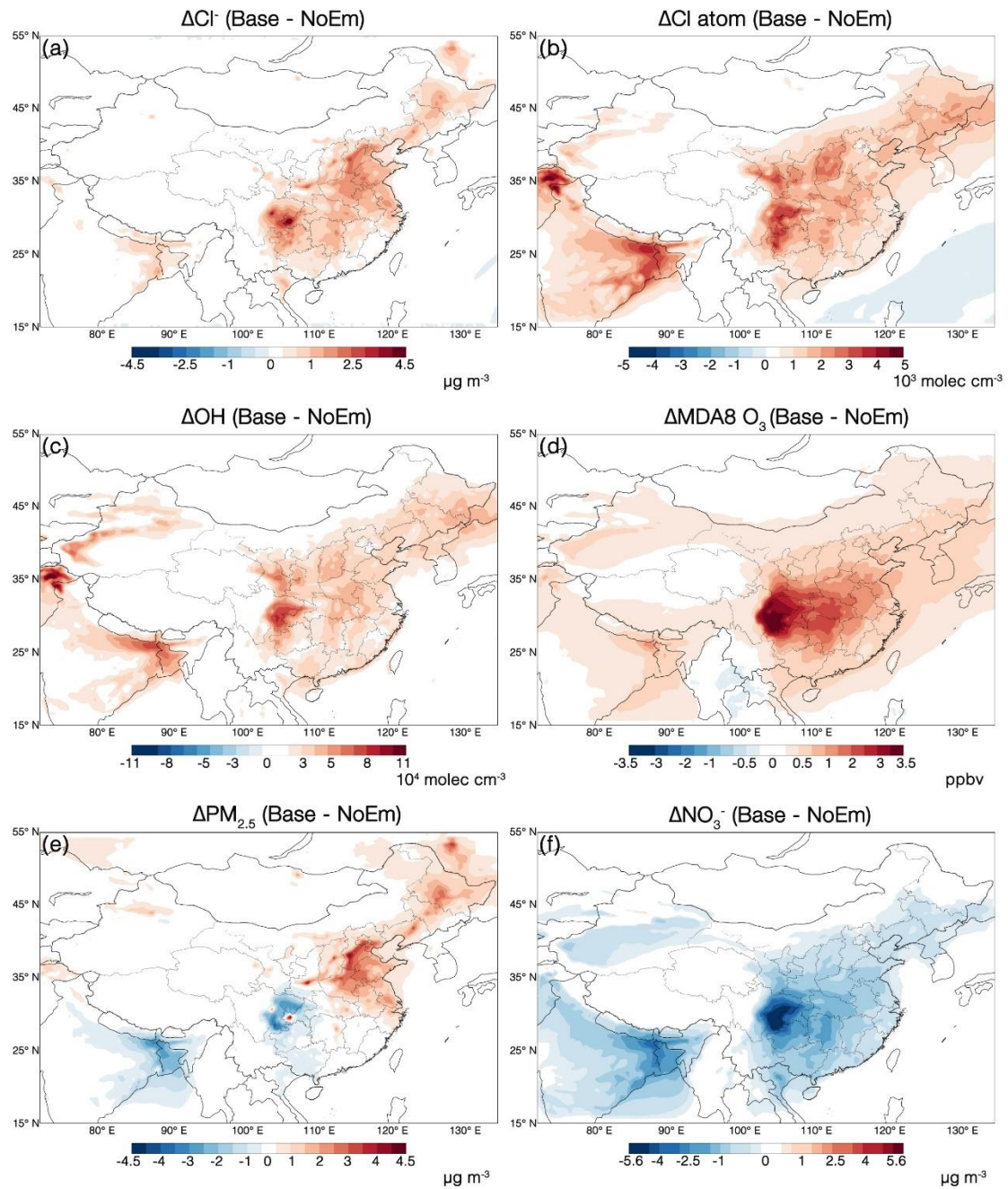
NoChem cases.

885



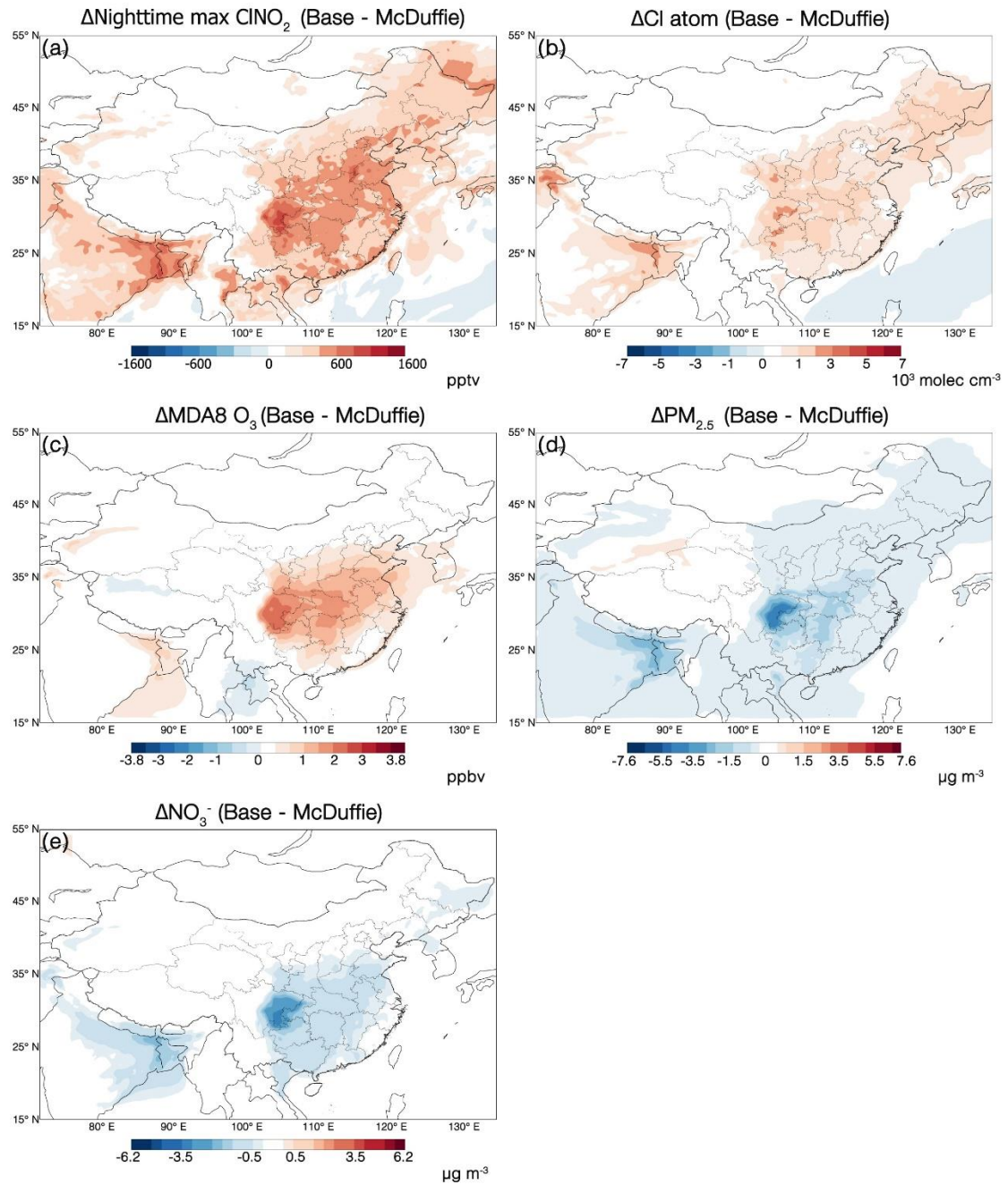
886

887 **Figure 6. Effects of the heterogeneous $\text{N}_2\text{O}_5 + \text{Cl}$ chemistry on annual mean surface concentrations of (a)**
 888 **nighttime max ClNO_2 , (b) Cl atom, (c) MDA8 O_3 and (d) PM $_{2.5}$ in China, estimated as the differences**
 889 **between the Base and NoHet cases.**



890
891
892
893
894

Figure 7. Effects of anthropogenic and biomass burning chlorine emissions on annual mean surface concentrations of (a) Cl^- , (b) Cl atom, (c) OH, (d) MDA8 O_3 , (e) $\text{PM}_{2.5}$ and (f) NO_3^- in China, estimated as the differences between the Base and NoEm cases.



895
 896
 897
 898
 899
 900
 901
 902
 903
 904
 905
 906

Figure 8. Effects of different parameterizations on annual mean surface concentrations of (a) nighttime max ClNO_2 , (b) Cl atom, (c) MDA8 O_3 , (d) PM $_{2.5}$, and (e) NO $_3^-$ in China, estimated as the differences between the Base and McDuffie cases.

907

Table 1. Chlorine emissions in China in the model.

| Sources | By default (Gg Cl a ⁻¹) | Updated in this study (Gg Cl a ⁻¹) |
|--|--|---|
| Sea salt Cl ⁻ | 6.5×10 ⁴ | 6.5×10 ⁴ |
| Anthropogenic HCl | 0 | 218 |
| Biomass burning HCl | 0 | 30 |
| Anthropogenic Cl ₂ | 0 | 8.9 |
| Anthropogenic Cl ⁻ | 0 | 379 |
| Biomass burning Cl ⁻ | 0 | 120 |
| CH ₃ Cl ^a | 3.8 | 3.8 |
| CH ₂ Cl ₂ ^a | 2.4 | 2.4 |
| CHCl ₃ ^a | 0.70 | 0.70 |

908 ^a: Sources are shown in terms of the chemical release (e.g. +Cl, +OH, +hv)

909

910

Table 2. Model setup of all simulation cases

| Cases | N ₂ O ₅ uptake ($\gamma_{N_2O_5}$) | ClNO ₂ production (ϕ_{ClNO_2}) | Other tropospheric chlorine chemistry | Anthropogenic and biomass burning inorganic chlorine emissions |
|----------|---|--|--|--|
| Base | Yu et al. (2020) | Yu et al. (2020) | Full | Yes |
| McDuffie | McDuffie et al. (2018a, 2018b) | McDuffie et al. (2018a, 2018b) | Full | Yes |
| NoEm | Yu et al. (2020) | Yu et al. (2020) | Full | None |
| NoHet | Yu et al. (2020) but with [Cl ⁻] = 0 | None | Full | Yes |
| NoChem | Yu et al. (2020) but with [Cl ⁻] = 0 | None | None | Yes |
| NoEmHet | Yu et al. (2020) but with [Cl ⁻] = 0 | None | Full | None |
| NoAll | Yu et al. (2020) but with [Cl ⁻] = 0 | None | None | None |

911

Table 3. Normalized mean bias (NMB) and correlation coefficients (*r*) between observed and simulated

913

MDA8 O₃ and PM_{2.5} concentrations during 2018 in China

| Species | Time | Base | | McDuffie | | NoEm | |
|---------------------|------------------|-------|----------|----------|----------|-------|----------|
| | | NMB | <i>r</i> | NMB | <i>r</i> | NMB | <i>r</i> |
| MDA8 O ₃ | Annual | -26% | 0.83 | -27% | 0.83 | -28% | 0.82 |
| | MAM ^a | -35% | 0.87 | -36% | 0.87 | -36% | 0.87 |
| | JJA ^b | -5.5% | 0.50 | -5.2% | 0.48 | -5.9% | 0.48 |
| | SON ^c | -24% | 0.79 | -26% | 0.78 | -28% | 0.76 |
| | DJF ^d | -49% | 0.81 | -53% | 0.80 | -54% | 0.80 |
| PM _{2.5} | Annual | 3.6% | 0.81 | 5.6% | 0.81 | 2.3% | 0.80 |
| | MAM | -6.3% | 0.52 | -4.9% | 0.53 | -6.2% | 0.52 |
| | JJA | 3.9% | 0.70 | 4.6% | 0.70 | 5.0% | 0.70 |
| | SON | 28% | 0.79 | 32% | 0.80 | 26% | 0.79 |
| | DJF | -4.3% | 0.82 | -2.6% | 0.82 | -7.9% | 0.82 |

914 ^a: March, April, and May (Spring)915 ^b: June, July, and August (Summer)916 ^c: September, October, and November (Autumn)917 ^d: December, January, and February (Winter)

918